

On Molecular Flow Velocity Meters

Maryam Farahnak-Ghazani, Mahtab Mirmohseni, and Masoumeh Nasiri-Kenari
Sharif University of Technology

Abstract

The concentration of molecules in the medium can provide us very useful information about the medium. In this paper, we use this information and design a molecular flow velocity meter using a molecule releasing node and a receiver that counts these molecules. We first assume M hypotheses according to M possible medium flow velocity values and an L -sample decoder at the receiver and obtain the flow velocity detector using maximum-a-posteriori (MAP) method. To analyze the performance of the proposed flow velocity detector, we obtain the error probability, and its Gaussian approximation and Chernoff information (CI) upper bound. We obtain the optimum sampling times which minimize the error probability and the sub-optimum sampling times which minimize the Gaussian approximation and the CI upper bound. When we have binary hypothesis, we show that the sub-optimum sampling times which minimize the CI upper bound are equal. When we have M hypotheses and $L \rightarrow \infty$, we show that the sub-optimum sampling times that minimize the CI upper bound yield to $\binom{M}{2}$ sampling times with $\binom{M}{2}$ weights. Then, we assume a randomly chosen constant flow velocity and obtain the MAP and minimum mean square error (MMSE) estimators for the L -sample receiver. We consider the mean square error (MSE) to investigate the error performance of the flow velocity estimators and obtain the Bayesian Cramer-Rao (BCR) and expected Cramer-Rao (ECR) lower bounds on the MSE of the estimators. Further, we obtain the sampling times which minimize the MSE. We show that when the flow velocity is in the direction of the connecting line between the releasing node and the receiver with uniform distribution for the magnitude of the flow velocity, and $L \rightarrow \infty$, two different sampling times are enough for the MAP estimator.

I. INTRODUCTION

Measuring medium flow velocity is an important problem with many applications; in molecular communication (MC) (for finding the channel state information), in industry (for abnormality detection), or in health-care (for measuring the blood flow velocity). The classic flow meters are mechanical devices which have certain applications based on the passing fluid, whose velocity is intended to be measured [1]. One of the important applications of flow meters is to measure the flow velocity of the blood. Blood flow velocity measurement is important in medical applications for monitoring heart function in order to

diagnose cardiovascular or other vascular diseases [2]. Some traditional blood flow measurement methods are indicator method [3]–[5], finger plethysmography [6], and electromagnetic based method [7]. In [3]–[5], the blood flow is measured by injecting indicator molecules and using mass balance equation. In [8], skin temperature measurement after receiving acupuncture manipulations is used to measure the blood flow. In [6], the finger blood flow is measured using finger plethysmography. These methods have low resolution. Methods with higher resolution, based on the microfluidic technology, are ultrasonic doppler method and laser doppler method [2].

In this paper, we use a molecular transmitter-receiver setup to measure the medium flow velocity. The molecules, which exist in the medium or released from a molecular source, can provide significant information, for instance, to design the molecular flow meter. Since the medium flow velocity affects the concentration of the received molecules, the flow velocity can be measured by monitoring the concentration changes. To this end, a molecular receiver can be employed to sense the concentration of the received molecules, and measure the flow velocity. This resembles a MC structure where a transmitter releases some molecules and a receiver senses the concentration of these molecules. MC has advantages in mediums that are more compatible with bio or chemical molecules like the human body or environmental applications. MC systems have been studied from different aspects, e.g., system modeling [9]–[12] capacity analysis [13]–[15], coding and modulation techniques [12], [16]–[18], inter-symbol interference (ISI) mitigation techniques [18]–[24], and channel estimation [25]–[27]. However, to the best of our knowledge, no work has studied the flow measurement in MC systems. The idea of sensing the concentration of molecules to measure the flow velocity was also used in the indicator method, which has been first introduced in 1824 by Hering to measure the blood flow velocity. In this method, some indicator molecules are injected to the blood vessel and sampled from other part of the vascular system. Then using the mass balance equation, the mean value of the blood flow is measured. In other words, the mean flow velocity is measured as the change in the fluid volume per unit time. When the change in the concentration of the indicator molecules is fixed, the mean flow velocity is written as the change in the indicator quantity per unit time divided by the change in the concentration of the indicator molecules. Hence, in this method, the steady state behavior of the system is considered. Further, the indicator method is just devoted to blood flow measurement and is studied in physiology. In this paper, using a MC analysis setup, we introduce a molecular flow meter, which can measure the flow velocity in any medium. Further, we consider the movement of each molecule and use the Fick's second law of diffusion to obtain the average value of the received concentration. Then, we determine the flow velocity by applying the conventional detection or estimation methods. As an important application, this flow meter can be used to design a new modulation method in MC, i.e., instead of encoding the information

on the properties of the released signal (concentration, type, or the release time of the molecules), we can encode the information on the properties of the medium specifically on the medium flow velocity, and at the receiver, we can decode the information by detecting the medium flow velocity. This modulation method can have advantages on the prior methods in the sense of simplicity of the transmitter.

The degrees of freedom in designing the proposed flow meter include the sensing times of the molecular receiver, which need to be optimized for better performance of the flow meter. For performance investigation, different metrics, such as the time it takes to detect a change in the velocity, and the error probability of the flow meter can be considered. The samples taken at the receiver are statistically dependent in general, and obtaining the optimum sampling times is a challenging work. Further, the restrictions in some receivers, like Ligand receivers which have memories, make the problem more challenging. We remark that the medium flow velocity that we want to measure may be a random process, which either exists in the medium or is intentionally generated for communication purposes. The medium flow velocity can take a real value in general. In that case, we should design an estimator to obtain its value. We first assume some possible discrete values for the flow velocity and design a flow velocity detector. For this purpose, we assume M hypothesis for the velocity (M different functions of time and location) and use hypotheses testing methods, [28], to detect the function. Finally, we assume a randomly chosen constant medium flow velocity and apply estimation methods, [28], to design a flow velocity estimator.

The design of a general flow meter requires knowing the exact statistics of the medium and the existing molecules in the medium, i.e., how molecules are generated and propagated. To study the effect of certain parameters on the performance of the flow meter, we need to simplify the reality by adopting a simple model. Hence, we make a few assumptions and study the effect of sampling time on the performance of the flow meter. We assume that the source of molecules is a node that releases some fixed molecules in some specific time instances, and the receiver is a transparent receiver, [29], with a sampling decoder, i.e., we assume that the receiver has a volume that counts the number of molecules inside its volume at some time instances. We consider an L -sample receiver and further assume that the samples at the receiver are statistically independent, which can be achieved if the samples are taken with some time apart. Also, we assume that there is no boundary condition on the medium, since obtaining the channel impulse response of the medium with time variant flow is a challenging work in presence of boundary conditions in the medium. Our main contributions are as follows:

- We design a molecular flow velocity meter, counting the number of arrived molecules affected by the flow of the medium. Our setup consists of a molecule releasing node and a receiver that samples the number of counted molecules.

- For the molecular flow velocity *detector*:
 - We obtain the optimum decision rule using maximum-a-posteriori (MAP) decision rule. For the one-sample decoder, we also obtain the optimum threshold.
 - We consider the performance analysis of the proposed detector. For this purpose, we derive the error probability, its Gaussian approximation, and Chernoff information (CI) upper bound on the error probability.
 - We obtain the optimum and sub-optimum sampling times by minimizing the error probability, its Gaussian approximation, and the CI upper bound. For $M = 2$, it is seen that the sub-optimum sampling times using CI upper bound are equal. For $M > 2$, when the number of samples, L , goes to infinity, it is seen that the sub-optimum sampling times yield to $\binom{M}{2}$ sampling times with $\binom{M}{2}$ weights.
- For the molecular flow velocity *estimator*:
 - We obtain the MAP estimator. For the one-sample receiver, we obtain a closed-form estimator.
 - We obtain the minimum mean square error (MMSE) estimator and further simplify the equations for the linear MMSE (LMMSE) estimator case.
 - We investigate the mean square error (MSE) of the above estimators. Further, we obtain the Bayesian and expected Cramer-Rao lower bounds on the MSE.
 - We obtain the optimum sampling times that minimize the MSE. When $L \rightarrow \infty$, it can be seen that the optimum sampling times for the MAP estimator yield to two sampling times with two weights.

The structure of the paper is as follows: In Section II, we describe the proposed molecular flow velocity detector/estimator setup. In Section III, we consider the flow velocity detector and obtain the MAP decision rule, and derive its performance. Further, we obtain the optimum and sub-optimum sampling times. In Section IV, we consider the flow velocity estimator and obtain the MAP estimator. Then, we obtain the estimation error and the optimum sampling times. The numerical results are given in Section V. Finally, in Section VI we conclude the paper.

Notation: Throughout the paper, vectors are shown with bold letters and their magnitudes, i.e., norm 2 of the vectors, are shown with non-bold letters.

II. MOLECULAR FLOW METER

We propose a molecular flow velocity meter to measure the medium flow velocity in a diffusion-based system. To do this, we assume that there is a node at the origin, which releases some constant number of molecules in some time instances, and there is a molecular receiver in point r_0 , which receives

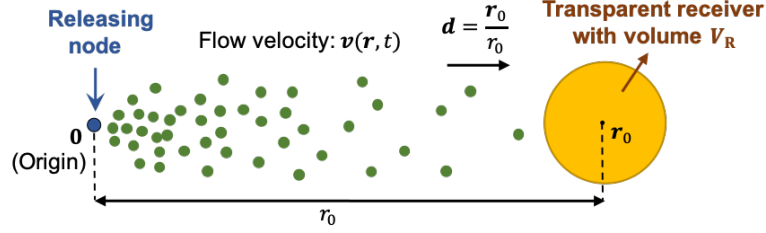


Fig. 1: The system model of the flow velocity meter

these molecules and computes the medium flow velocity. Hence, \mathbf{r}_0 is a vector which connects the releasing node to the receiver. We note the direction of this connecting line with \mathbf{d} and its value with r_0 . Hence, $\mathbf{r}_0 = r_0 \mathbf{d}$ (see Fig. 1). The releasing node may have different behaviors. Assume $g(\mathbf{r}, t)$ be the concentration of released molecules at point \mathbf{r} and in time t . In the following, we mention some of the possibilities of the releasing node:

i) **Burst releasing:** a burst of molecules, noted by ζ , is released at time instance $t = t_r$. For this releasing node we have $g(\mathbf{r}, t) = \zeta \delta(t - t_r) \delta(\mathbf{r})$.

ii) **Pulse releasing:** the molecules with rate γ are constantly released starting at $t = t_r$. For this releasing node we have $g(\mathbf{r}, t) = \gamma \delta(\mathbf{r}) u(t - t_r)$.

In this paper, we assume the *burst releasing* node.

Channel model: For the diffusion of molecules, we use the deterministic model based on Fick's second law of diffusion. According to this model, the concentration of molecules at point \mathbf{r} and in time t , noted as $c(\mathbf{r}, t)$, in a medium with flow velocity $\mathbf{v}(\mathbf{r}, t)$ satisfies the following equation:

$$\frac{\partial}{\partial t} c(\mathbf{r}, t) + \nabla \cdot (\mathbf{v}(\mathbf{r}, t) c(\mathbf{r}, t)) = D \nabla^2 c(\mathbf{r}, t) + g(\mathbf{r}, t), \quad (1)$$

where D is the diffusion coefficient of molecules. When the medium flow is location invariant, i.e., $\mathbf{v}(\mathbf{r}, t) = \mathbf{v}(t)$ (which means that the flow velocity is the same in every point of the medium and the change in the flow velocity of one point propagates to other points quickly), the diffusion equation in (1), reduces to:

$$\frac{\partial}{\partial t} c(\mathbf{r}, t) + \mathbf{v}(t) \cdot \nabla c(\mathbf{r}, t) = D \nabla^2 c(\mathbf{r}, t) + g(\mathbf{r}, t). \quad (2)$$

Reception model: We assume that the receiver is modeled by a sphere in 3-D with volume V_R (radius r_R) and consider a transparent receiver, i.e., the receiver can perfectly count all molecules that fall into its volume. We assume an L -sample decoder at the receiver, which means that the receiver counts the number of received molecules in L time instances in each time slot, denoted by $t_l, l = 1, \dots, L$. Denoting the mean number of received molecules in the l -th sample as λ_l , the number of molecules counted by the receiver (noted by Y_l) follows a Poisson distribution with parameter λ_l , i.e., $Y_l \sim \text{Pois}(\lambda_l)$ [29]. λ_l can

be obtained from $c(\mathbf{r}, t)$ as $\lambda_l = V_R c(\mathbf{0}, t_l)$. For simplicity of analysis, we assume that the observations Y_1, \dots, Y_L are independent. This assumption can be made if the samples are taken with some time apart, i.e., the sampling times have sufficient distance from each other [30].

In the following, we obtain the channel impulse response and hence $c(\mathbf{r}, t)$, and Λ_l , when the medium flow velocity is location invariant (i.e., $\mathbf{v}(\mathbf{r}, t) = \mathbf{v}(t)$).

The impulse response of this system, $h(\mathbf{r}, t)$, is defined as the concentration of molecules at point \mathbf{r} and in time t , which is the solution of (2), for input $g(\mathbf{r}, t) = \delta(\mathbf{r})\delta(t - t_r)$. The channel impulse response is obtained in [31] using Ito's calculus for the mean location of molecules, i.e., if $m(t)$ is the mean location of molecules, using Ito's calculus we have $m(t) = \int_{t_r}^t \mathbf{v}(\tau) d\tau$. Hence, for 3-D diffusion,

$$h(\mathbf{r}, t) = \frac{1[t > t_r]}{(4\pi D(t - t_r))^{3/2}} \exp\left(-\frac{(\|\mathbf{r} - m(t)\|^2)}{4D(t - t_r)}\right).$$

An alternative method to obtain the channel impulse response is provided in Lemma 1.

Lemma 1. *The response of the diffusion channel with time variant flow velocity $\mathbf{v}(t)$ to input signal $g(\mathbf{r}, t) = \delta(\mathbf{r})\delta(t - t_r)$ for 3-D diffusion can be obtained as follows:*

$$h(\mathbf{r}, t) = h_0\left(\mathbf{r} - \int_{t_r}^t \mathbf{v}(\tau) d\tau, t\right), \quad (3)$$

where

$$h_0(\mathbf{r}, t) = \frac{1[t > t_r]}{(4\pi D(t - t_r))^{3/2}} \exp\left(-\frac{(\|\mathbf{r}\|^2)}{4D(t - t_r)}\right). \quad (4)$$

Proof. We obtain the response of eq. (2) for $g(\mathbf{r}, t) = \delta(\mathbf{r})\delta(t - t_r)$, i.e.,

$$\frac{\partial}{\partial t} h(\mathbf{r}, t) + \mathbf{v}(t) \cdot \nabla h(\mathbf{r}, t) = D \nabla^2 h(\mathbf{r}, t) + \delta(\mathbf{r})\delta(t - t_r). \quad (5)$$

Assume $h_0(\mathbf{r}, t)$ is the response of the channel without medium flow ($\mathbf{v}(t) = 0$) to input $g(\mathbf{r}, t) = \delta(t - t_r)\delta(\mathbf{r})$. Hence, $h_0(\mathbf{r}, t)$ must satisfy the following equation:

$$\frac{\partial}{\partial t} h_0(\mathbf{r}, t) = D \nabla^2 h_0(\mathbf{r}, t) + \delta(\mathbf{r})\delta(t - t_r). \quad (6)$$

The green function is the solution of (6) as follows [32]:

$$h_0(\mathbf{r}, t) = \frac{1[t > t_r]}{(4\pi D(t - t_r))^{3/2}} \exp\left(-\frac{(\|\mathbf{r}\|^2)}{4D(t - t_r)}\right). \quad (7)$$

We show that $h(\mathbf{r}, t) = h_0(\mathbf{r}^*, t)$, where $\mathbf{r}^* = \mathbf{r} - \int_{t_r}^t \mathbf{v}(\tau) d\tau$, satisfies eq. (5). We have

$$\frac{\partial}{\partial t} h(\mathbf{r}, t) = \nabla h_0(\mathbf{r}^*, t) \cdot \frac{\partial \mathbf{r}^*}{\partial t} + \frac{\partial h_0}{\partial t}(\mathbf{r}^*, t) = \nabla h_0(\mathbf{r}^*, t) \cdot (-\mathbf{v}(t)) + \frac{\partial h_0}{\partial t}(\mathbf{r}^*, t), \quad (8)$$

$$\nabla h(\mathbf{r}, t) = \nabla h_0(\mathbf{r}^*, t), \quad (9)$$

$$\nabla^2 h(\mathbf{r}, t) = \nabla^2 h_0(\mathbf{r}^*, t). \quad (10)$$

Hence,

$$\begin{aligned}
\frac{\partial}{\partial t}h(\mathbf{r}, t) + \mathbf{v}(t) \cdot \nabla h(\mathbf{r}, t) &\stackrel{(a)}{=} \nabla h_0(\mathbf{r}^*, t) \cdot \frac{\partial \mathbf{r}^*}{\partial t} + \frac{\partial h_0}{\partial t}(\mathbf{r}^*, t) \\
&= \nabla h_0(\mathbf{r}^*, t) \cdot (-\mathbf{v}(t)) + \frac{\partial h_0}{\partial t}(\mathbf{r}^*, t) + \mathbf{v}(t) \cdot \nabla h_0(\mathbf{r}^*, t) \\
&= \frac{\partial}{\partial t}h_0(\mathbf{r}^*, t) \stackrel{(b)}{=} D\nabla^2 h_0(\mathbf{r}^*, t) + \delta(\mathbf{r})\delta(t - t_r) \\
&\stackrel{(c)}{=} D\nabla^2 h(\mathbf{r}, t) + \delta(\mathbf{r})\delta(t - t_r).
\end{aligned} \tag{11}$$

where (a) is due to (8) and (9), (b) is due to (6), and (c) is due to (10). Hence, $h(\mathbf{r}, t) = h_0(\mathbf{r}^*, t)$ is the response of the system with location invariant medium flow velocity to input $g(\mathbf{r}, t) = \delta(t - t_r)\delta(\mathbf{r})$ given in (5). \square

Now, using the channel impulse response we obtain Λ_l . Assuming the burst releasing node, we have $c(\mathbf{r}, t) = \zeta h(\mathbf{r}, t)$ and hence, $\Lambda_l = V_R c(\mathbf{r}_0, t_l) = \zeta V_R h(\mathbf{r}_0, t_l)$. Thus, according to Lemma 1, we obtain

$$\Lambda_l = \zeta V_R h_0\left(\mathbf{r}_0 - \int_{t_r}^{t_l} \mathbf{v}(\tau) d\tau, t_l\right). \tag{12}$$

III. FLOW VELOCITY DETECTOR WITH L -SAMPLE RECEIVER

Consider M hypotheses H_0, H_1, \dots, H_{M-1} corresponding to the flow velocities $\mathbf{v}_0(\mathbf{r}, t), \mathbf{v}_1(\mathbf{r}, t), \dots, \mathbf{v}_{M-1}(\mathbf{r}, t)$. We denote the mean number of counted molecules at the receiver in sampling time t_l for the hypothesis H_i as $\lambda_{i,l}, i = 0, \dots, M-1, l = 1, \dots, L$. For the location invariant flow velocity and for the transparent receiver, from (12), we have $\lambda_{i,l} = V_R \zeta h_0\left(\mathbf{r}_0 - \int_{t_r}^{t_l} \mathbf{v}_i(\tau) d\tau, t_l\right)$. We assume that the prior probabilities of the hypotheses are equal, i.e., $P(H_i) = \frac{1}{M}, i = 0, \dots, M-1$.

Lemma 2. (Optimum decision rule) For a molecular flow velocity detector with M hypotheses, and L -sample decoder at the receiver, the optimum MAP decision rule is obtained as

$$\hat{i} = \arg \max_{i \in \{0, \dots, M-1\}} \sum_{l=1}^L y_l \ln(\lambda_{i,l}) - \lambda_{i,l}, \tag{13}$$

Proof. Using MAP decision rule with equal prior probabilities for the hypotheses, we have

$$\hat{i} = \arg \max_{i \in \{0, \dots, M-1\}} P(y_1, y_2, \dots, y_L | H_i). \tag{14}$$

For the independent observations, $P(y_1, y_2, \dots, y_L | H_i) = \prod_{l=1}^L P(y_l | H_i)$. The conditional probability distribution of Y_l given H_i assuming counting noise at the receiver is $\text{Pois}(\lambda_{i,l})$ for $i = 0, \dots, M-1, l = 1, \dots, L$. Hence,

$$\hat{i} = \arg \max_{i \in \{0, \dots, M-1\}} \prod_{l=1}^L \frac{(\lambda_{i,l})^{y_l} \exp(-\lambda_{i,l})}{y_l!} = \arg \max_{i \in \{0, \dots, M-1\}} \prod_{l=1}^L (\lambda_{i,l})^{y_l} \exp(-\lambda_{i,l}) \tag{15}$$

$$= \arg \max_{i \in \{0, \dots, M-1\}} \sum_{l=1}^L y_l \ln(\lambda_{i,l}) - \lambda_{i,l}.$$

□

Corollary 2.1. For binary hypothesis, the optimum decision rule is simply obtained as

$$\sum_{l=1}^L w_l y_l \underset{H_1}{\overset{H_0}{\geq}} \beta, \quad (16)$$

where $w_l = \ln(\frac{\lambda_{0,l}}{\lambda_{1,l}})$ and $\beta = \sum_{l=1}^L (\lambda_{0,l} - \lambda_{1,l})$.

Corollary 2.2. For binary hypothesis and one-sample decoder, the optimum decision rule is a simple threshold rule as $y_1 \underset{H_1}{\overset{H_0}{\geq}} \mathcal{T}$, with the threshold

$$\mathcal{T} = \frac{\lambda_{0,1} - \lambda_{1,1}}{\ln(\frac{\lambda_{0,1}}{\lambda_{1,1}})}. \quad (17)$$

Lemma 3. (Error probability) The error probability in detecting the flow velocity, with M hypotheses and L -sample decoder at the receiver, is obtained as follows:

$$P_e = 1 - \frac{1}{M} \sum_{i=0}^{M-1} \sum_{\substack{y_1, \dots, y_L=0, \\ \sum_{l=1}^L w_{i,j,l} y_l > \beta_{i,j}, j=0, \dots, M-1, j \neq i}}^{\infty} \prod_{l=1}^L \frac{(\lambda_{i,l})^{y_l} \exp(-\lambda_{i,l})}{y_l!}, \quad (18)$$

where $w_{i,j,l} = \ln(\frac{\lambda_{i,l}}{\lambda_{j,l}})$ and $\beta_{i,j} = \sum_{l=1}^L (\lambda_{i,l} - \lambda_{j,l})$.

Proof. Let $R_i = \prod_{l=1}^L (\lambda_{i,l})^{y_l} \exp(-\lambda_{i,l})$. Using the optimum decision rule given in (13), the error probability can be obtained as

$$\begin{aligned} P_e &= \frac{1}{M} \sum_{i=0}^{M-1} [1 - \text{P}\{\cap_{j=0, \dots, M-1, j \neq i} R_i > R_j | H_i\}] \\ &= 1 - \frac{1}{M} \sum_{i=0}^{M-1} \sum_{\substack{y_1, \dots, y_L=0, \\ R_i > R_j, j=0, \dots, M-1, j \neq i}}^{\infty} \text{P}(y_1, \dots, y_L | H_i) \\ &= 1 - \frac{1}{M} \sum_{i=0}^{M-1} \sum_{\substack{y_1, \dots, y_L=0, \\ R_i > R_j, j=0, \dots, M-1, j \neq i}}^{\infty} \prod_{l=1}^L \text{P}(Y_l = y_l | H_i). \end{aligned} \quad (19)$$

The condition $R_i > R_j$ reduces to $w_{i,j,l} y_l > \beta_{i,j}$, where $w_{i,j,l} = \ln(\frac{\lambda_{i,l}}{\lambda_{j,l}})$ and $\beta_{i,j} = \sum_{l=1}^L (\lambda_{i,l} - \lambda_{j,l})$ (similar to (16)), and hence, P_e simplifies to

$$P_e = 1 - \frac{1}{M} \sum_{i=0}^{M-1} \sum_{\substack{y_1, \dots, y_L=0, \\ \sum_{l=1}^L w_{i,j,l} y_l > \beta_{i,j}, j=0, \dots, M-1, j \neq i}}^{\infty} \prod_{l=1}^L \text{P}(Y_l = y_l | H_i). \quad (20)$$

Now, by substituting the Poisson distribution for $\text{P}(Y_l = y_l | H_i)$, we obtain (18). □

Corollary 3.1. For binary hypothesis, the error probability is simplified as:

$$P_e = \frac{1}{2} \left[1 - \sum_{\substack{y_1, \dots, y_L=0, \\ \sum_{l=1}^L w_l y_l > \beta}}^{\infty} \left(\prod_{l=1}^L \frac{(\lambda_{0,l})^{y_l} \exp(-\lambda_{0,l})}{y_l!} - \prod_{l=1}^L \frac{(\lambda_{1,l})^{y_l} \exp(-\lambda_{1,l})}{y_l!} \right) \right], \quad (21)$$

where w_l and β are defined in Corollary 2.1. Further, the Gaussian approximation on the error probability is obtained as

$$P_e \approx P_{e,G} = \frac{1}{2} \left[1 - Q\left(\frac{\beta - \sum_{l=1}^L w_l \lambda_{0,l}}{\sqrt{\sum_{l=1}^L w_l^2 \lambda_{0,l}}}\right) + Q\left(\frac{\beta - \sum_{l=1}^L w_l \lambda_{1,l}}{\sqrt{\sum_{l=1}^L w_l^2 \lambda_{1,l}}}\right) \right], \quad (22)$$

where $Q(x) = \frac{1}{2\pi} \int_x^{\infty} \exp(-\frac{u^2}{2}) du$.

Proof. The proof is provided in Appendix A. □

Corollary 3.2. For binary hypothesis and one-sample decoder, the error probability reduces to

$$P_e = \frac{1}{2} \left[1 - \sum_{y_1=0}^{\lfloor \mathcal{T} \rfloor} \frac{(\lambda_{0,1})^{y_1} \exp(-\lambda_{0,1}) - (\lambda_{1,1})^{y_1} \exp(-\lambda_{1,1})}{y_1!} \right], \quad (23)$$

for $\lambda_{0,1} > \lambda_{1,1}$, where \mathcal{T} is defined in Corollary 2.2. Further, the Gaussian approximation on the error probability is obtained as

$$P_e = \frac{1}{2} \left[1 + Q\left(\frac{\mathcal{T} - \lambda_{0,1}}{\sqrt{\lambda_{0,1}}}\right) - Q\left(\frac{\mathcal{T} - \lambda_{1,1}}{\sqrt{\lambda_{1,1}}}\right) \right], \quad (24)$$

where $Q(x)$ is defined in Corollary 3.1.

In the following, we obtain the Chernoff information (CI) upper bound on the error probability for the MAP detector [33], [34]. Chernoff uses the inequality

$$\min(a, b) \leq a^s b^{1-s} \quad \forall s \in [0, 1], \quad (25)$$

to upper bound the error probability of the MAP detector.

Lemma 4. (CI upper bound on error probability) The CI upper bound on the error probability with M hypotheses and L -sample decoder is obtained as follows:

$$P_e \leq P_{e,CI} = \frac{M-1}{2} \max_{\substack{i_1, i_2 \in \{0, \dots, M-1\}, \\ i_1 \neq i_2}} \min_{s_{i_1, i_2} \in [0, 1]} \exp(-D_{i_1, i_2}(s_{i_1, i_2})), \quad (26)$$

where $D_{i_1, i_2}(s_{i_1, i_2}) = \sum_{l=1}^L [\lambda_{i_1, l} s_{i_1, i_2} + \lambda_{i_2, l} (1 - s_{i_1, i_2}) - \lambda_{i_1, l}^{s_{i_1, i_2}} \lambda_{i_2, l}^{1-s_{i_1, i_2}}]$. The optimum value of s_{i_1, i_2} is the solution of the following equation:

$$\sum_{l=1}^L \left[\lambda_{i_1, l} - \lambda_{i_2, l} - \lambda_{i_1, l} \left(\frac{\lambda_{i_1, l}}{\lambda_{i_2, l}} \right)^{s_{i_1, i_2}} \ln \left(\frac{\lambda_{i_1, l}}{\lambda_{i_2, l}} \right) \right] = 0. \quad (27)$$

Proof. The error probability of the MAP detector with M hypotheses in (19) can also be written as

$$P_e = \frac{1}{M} \sum_{i=0}^{M-1} \text{P}\{\cup_{j=0, \dots, M-1, j \neq i} R_i < R_j | H_i\}. \quad (28)$$

Now, we upper bound the error probability as follows:

$$\begin{aligned} P_e &\stackrel{(a)}{\leq} \frac{1}{M} \sum_{i=0}^{M-1} \sum_{\substack{j=0, \\ j \neq i}}^{M-1} \text{P}\{R_i < R_j | H_i\} \\ &= \frac{1}{M} \sum_{i=0}^{M-1} \sum_{\substack{j=0, \\ j \neq i}}^{M-1} \sum_{y_1, \dots, y_L=0}^{\infty} \mathbf{1}\{\text{P}(y_1, \dots, y_L | H_i) < \text{P}(y_1, \dots, y_L | H_j)\} \text{P}(y_1, \dots, y_L | H_i) \\ &= \frac{1}{M} \sum_{\substack{i_1, i_2 \in \{0, \dots, M-1\}, \\ i_1 \neq i_2}} \sum_{y_1, \dots, y_L=0}^{\infty} \min\{\text{P}(y_1, \dots, y_L | H_{i_1}), \text{P}(y_1, \dots, y_L | H_{i_2})\} \\ &\stackrel{(b)}{\leq} \frac{1}{M} \sum_{\substack{i_1, i_2 \in \{0, \dots, M-1\}, \\ i_1 \neq i_2}} \sum_{y_1, \dots, y_L=0}^{\infty} \text{P}(y_1, \dots, y_L | H_{i_1})^{s_{i_1, i_2}} \text{P}(y_1, \dots, y_L | H_{i_2})^{1-s_{i_1, i_2}} \\ &\stackrel{(c)}{=} \frac{1}{M} \sum_{\substack{i_1, i_2 \in \{0, \dots, M-1\}, \\ i_1 \neq i_2}} \prod_{l=1}^L \sum_{y_l=0}^{\infty} \text{P}(y_l | H_{i_1})^{s_{i_1, i_2}} \text{P}(y_l | H_{i_2})^{1-s_{i_1, i_2}} \\ &\stackrel{(d)}{=} \frac{1}{M} \sum_{\substack{i_1, i_2 \in \{0, \dots, M-1\}, \\ i_1 \neq i_2}} \exp\left(-\sum_{l=1}^L (\lambda_{i_1, l} s_{i_1, i_2} + \lambda_{i_2, l} (1 - s_{i_1, i_2}) - \lambda_{i_1, l}^{s_{i_1, i_2}} \lambda_{i_2, l}^{1-s_{i_1, i_2}})\right) \\ &\stackrel{(e)}{\leq} \frac{1}{M} \binom{M}{2} \max_{\substack{i_1, i_2 \in \{0, \dots, M-1\}, \\ i_1 \neq i_2}} \exp\left(-\sum_{l=1}^L (\lambda_{i_1, l} s_{i_1, i_2} + \lambda_{i_2, l} (1 - s_{i_1, i_2}) - \lambda_{i_1, l}^{s_{i_1, i_2}} \lambda_{i_2, l}^{1-s_{i_1, i_2}})\right), \end{aligned} \quad (29)$$

where (a) is due to the union bound, (b) is due to eq. (25), (c) is due to assuming independent observations at the receiver, (d) is due to Poisson distribution for observations, i.e., $\text{P}(y_l | H_i) = \frac{(\lambda_{i, l})^{y_l} \exp(-\lambda_{i, l})}{y_l!}$, $i \in \{0, \dots, M-1\}$, $l \in \{1, \dots, L\}$, and (e) is due to substituting the maximum term for each term of the summation. Since the bound holds for all values of $s_{i_1, i_2} \in (0, 1)$, it also holds for the optimum values of s_{i_1, i_2} , which is obtained by minimizing $\exp(-D_{i_1, i_2}(s_{i_1, i_2}))$, i.e., maximizing $D_{i_1, i_2}(s_{i_1, i_2})$ with respect to s_{i_1, i_2} . Hence, we obtain the upper bound as (26). The optimum s_{i_1, i_2} is obtained by minimizing $\exp(-D_{i_1, i_2}(s_{i_1, i_2}))$, i.e., maximizing $D_{i_1, i_2}(s_{i_1, i_2})$ with respect to s_{i_1, i_2} . Hence s_{i_1, i_2}^* is the solution of $\frac{d}{ds_{i_1, i_2}} D_{i_1, i_2}(s_{i_1, i_2}) = 0$ which can be simplified as (27). \square

There is no closed form solution for the optimum value of s_{i_1, i_2} in (27). In Corollary 4.1, we use Holder's inequality, [35], to simplify the bound and obtain a closed form solution for the sub-optimum value of s_{i_1, i_2} .

Corollary 4.1. *Using Holder's inequality on the CI upper bound, the error probability is upper bounded as follows:*

$$P_e \leq P_{e,HCI} = \frac{M-1}{2} \max_{\substack{i_1, i_2 \in \{0, \dots, M-1\}, \\ i_1 \neq i_2}} \min_{s_{i_1, i_2} \in [0, 1]} \exp(-K_{i_1, i_2}(s_{i_1, i_2})), \quad (30)$$

where $K(s_{i_1, i_2}) = (\sum_{l=1}^L \lambda_{i_1, l})s_{i_1, i_2} + (\sum_{l=1}^L \lambda_{i_2, l})(1 - s_{i_1, i_2}) - (\sum_{l=1}^L \lambda_{i_1, l})^{s_{i_1, i_2}} (\sum_{l=1}^L \lambda_{i_2, l})^{1-s_{i_1, i_2}}$. The optimum value of s_{i_1, i_2} is obtained as

$$s_{i_1, i_2}^* = \frac{\ln(\frac{\sum_{l=1}^L \lambda_{i_1, l}}{\sum_{l=1}^L \lambda_{i_2, l}} - 1) - \ln \ln(\frac{\sum_{l=1}^L \lambda_{i_1, l}}{\sum_{l=1}^L \lambda_{i_2, l}})}{\ln(\frac{\sum_{l=1}^L \lambda_{i_1, l}}{\sum_{l=1}^L \lambda_{i_2, l}})}. \quad (31)$$

Proof. The proof is provided in Appendix B. □

Corollary 4.2. *For binary hypothesis, the CI upper bound in (26) reduces to*

$$P_e \leq P_{e,u} = \frac{1}{2} \min_{s \in (0, 1)} \exp(-D(s)), \quad (32)$$

where $D(s) = \sum_{l=1}^L (\lambda_{0,l}s + \lambda_{1,l}(1-s) - \lambda_{0,l}^s \lambda_{1,l}^{1-s})$. The optimum value of s is the solution of the following equation:

$$\sum_{l=1}^L [\lambda_{0,l} - \lambda_{1,l} - \lambda_{0,l} (\frac{\lambda_{0,l}}{\lambda_{1,l}})^s \ln(\frac{\lambda_{0,l}}{\lambda_{1,l}})] = 0. \quad (33)$$

Corollary 4.3. *For binary hypothesis and one-sample decoder, i.e., $L=1$, the CI upper bound in (26) is simplified as*

$$P_e \leq P_{e,u} = \frac{1}{2} \exp(-(\lambda_{0,1}s^* + \lambda_{1,1}(1-s^*) - \lambda_{0,1}^{s^*} \lambda_{1,1}^{1-s^*})), \quad (34)$$

where

$$s^* = \frac{\ln(\frac{\lambda_{0,1}}{\lambda_{1,1}} - 1) - \ln \ln(\frac{\lambda_{0,1}}{\lambda_{1,1}})}{\ln(\frac{\lambda_{0,1}}{\lambda_{1,1}})}. \quad (35)$$

Optimum and Sub-optimum sampling times: The optimum sampling times, which minimize the error probability, are

$$[t_1^*, t_2^*, \dots, t_L^*] = \arg \min_{t_1, t_2, \dots, t_L} P_e, \quad (36)$$

where P_e is given in (18). Since the above optimization problem is hard to solve in general case, the optimum sampling times should be obtained numerically. We use the Gaussian approximation and CI upper bound on the error probability and obtain the sub-optimum sampling times as the solutions of the following optimization problems:

$$[t_{1,G}, t_{2,G}, \dots, t_{L,G}] = \arg \min_{t_1, t_2, \dots, t_L} P_{e,G}, \quad (37)$$

$$[t_{1,\text{CI}}, t_{2,\text{CI}}, \dots, t_{L,\text{CI}}] = \arg \min_{t_1, t_2, \dots, t_L} P_{e,\text{CI}} = \arg \max_{t_1, t_2, \dots, t_L} \min_{i_1, i_2 \in \{0, \dots, M-1\}, s_{i_1, i_2}} \max_{i_1 \neq i_2} D_{i_1, i_2}(s_{i_1, i_2}), \quad (38)$$

where $P_{e,G}$ is defined in (22) and $P_{e,\text{CI}}$, D_{i_1, i_2} are defined in (26). In Lemma 5, using the extension of Caratheodory's theorem [36], we obtain the sub-optimum sampling times using CI upper bound, when $L \rightarrow \infty$, in Lemma 6, we obtain the sub-optimum sampling times for binary hypothesis using Gaussian approximation of the error probability, and in Lemma 7, we obtain the sub-optimum sampling times for binary hypothesis using CI upper bound.

Lemma 5. (Sub-optimum sampling times using CI upper bound when $L \rightarrow \infty$) The sub-optimum sampling times using CI upper bound are $\binom{M}{2}$ times, $t_l, l = 1, \dots, \binom{M}{2}$, with weight w_l , i.e., Lw_l sampling times are equal to t_l , where t_l s and w_l s are obtained from the following optimization problem:

$$\max_{w_1, w_2, \dots, w_{\binom{M}{2}}} \max_{t_1, t_2, \dots, t_{\binom{M}{2}}} \min_{i_1, i_2 \in \{0, \dots, M-1\}, s_{i_1, i_2}} \max_{i_1 \neq i_2} \sum_{l=1}^{\binom{M}{2}} w_l f_{i_1, i_2}(t_l, s_{i_1, i_2}), \quad (39)$$

where $f_{i_1, i_2}(t_l, s_{i_1, i_2}) = \lambda_{i_1, l} s_{i_1, i_2} + \lambda_{i_2, l} (1 - s_{i_1, i_2}) - \lambda_{i_1, l}^{s_{i_1, i_2}} \lambda_{i_2, l}^{1-s_{i_1, i_2}}$.

Proof. To obtain the optimum sampling times using CI upper bound in (26), we must solve

$$\max_{t_1, t_2, \dots, t_L} \min_{i_1, i_2 \in \{0, \dots, M-1\}, s_{i_1, i_2}} \max_{i_1 \neq i_2} D_{i_1, i_2}(s_{i_1, i_2}), \quad (40)$$

where $D_{i_1, i_2}(s_{i_1, i_2}) = \sum_{l=1}^L \lambda_{i_1, l} s_{i_1, i_2} + \lambda_{i_2, l} (1 - s_{i_1, i_2}) - \lambda_{i_1, l}^{s_{i_1, i_2}} \lambda_{i_2, l}^{1-s_{i_1, i_2}}$. $\lambda_{i, l}$ is a function of the sampling time t_l . Hence, $D_{i_1, i_2}(s_{i_1, i_2}) = \sum_{l=1}^L f_{i_1, i_2}(t_l, s_{i_1, i_2})$. For each sampling time t_l , $l = 1, \dots, L$, $\mathbf{a}_l = (f_{0,1}(t_l, s_{0,1}), f_{0,2}(t_l, s_{0,2}), \dots, f_{M-1, M}(t_l, s_{M-1, M}))$ is a point in $\mathbb{R}^{\binom{M}{2}}$. The average of these points is

$$\frac{1}{L} \sum_{l=1}^L \mathbf{a}_l = \left(\frac{1}{L} \sum_{l=1}^L f_{0,1}(t_l, s_{0,1}), \frac{1}{L} \sum_{l=1}^L f_{0,2}(t_l, s_{0,2}), \dots, \frac{1}{L} \sum_{l=1}^L f_{M-1, M}(t_l, s_{M-1, M}) \right).$$

When $L \rightarrow \infty$, we have infinite points and the average point is in the convex hull of a set in $\mathbb{R}^{\binom{M}{2}}$. Using the extension of Caratheodory's theorem for connected sets, [36], every point in the convex hull of a set T in \mathbb{R}^n can be expressed as a convex combination of at most n points of T . Here, $n = \binom{M}{2}$, and we denote these $\binom{M}{2}$ points by $\mathbf{b}_l = (f_{0,1}(t'_l, s_{0,1}), f_{0,2}(t'_l, s_{0,2}), \dots, f_{M-1, M}(t'_l, s_{M-1, M}))$, $l = 1, \dots, \binom{M}{2}$. Hence, $\frac{1}{L} \sum_{l=1}^L \mathbf{a}_l = \sum_{l=1}^{\binom{M}{2}} w_l \mathbf{b}_l$. Thus, for a fixed s_{i_1, i_2} , we have

$$\frac{1}{L} \sum_{l=1}^L f_{i_1, i_2}(t_l, s_{i_1, i_2}) = \sum_{l=1}^{\binom{M}{2}} w_l f_{i_1, i_2}(t'_l, s_{i_1, i_2}), \quad i_1, i_2 \in \{0, \dots, M-1\}, \quad i_1 \neq i_2, \quad (41)$$

and from (40), we can conclude

$$\lim_{L \rightarrow \infty} \max_{t_1, t_2, \dots, t_L} \min_{i_1, i_2 \in \{0, \dots, M-1\}, s_{i_1, i_2}} \frac{1}{L} \sum_{l=1}^L f_{i_1, i_2}(t_l, s_{i_1, i_2}) =$$

$$\max_{w_1, w_2, \dots, w_{\binom{M}{2}}} \max_{t'_1, t'_2, \dots, t'_{\binom{M}{2}}} \min_{\substack{i_1, i_2 \in \{0, \dots, M-1\}, \\ i_1 \neq i_2}} w_l f_{i_1, i_2}(t'_l, s_{i_1, i_2}). \quad (42)$$

Now, we are required to show the following expression:

$$\lim_{L \rightarrow \infty} \max_{t_1, t_2, \dots, t_L} \min_{\substack{i_1, i_2 \in \{0, \dots, M-1\}, \\ i_1 \neq i_2}} \max_{s_{i_1, i_2}} \frac{1}{L} \sum_{l=1}^L f_{i_1, i_2}(t_l, s_{i_1, i_2}) = \quad (43a)$$

$$\max_{w_1, w_2, \dots, w_{\binom{M}{2}}} \max_{t'_1, t'_2, \dots, t'_{\binom{M}{2}}} \min_{\substack{i_1, i_2 \in \{0, \dots, M-1\}, \\ i_1 \neq i_2}} \max_{s_{i_1, i_2}} \sum_{l=1}^{\binom{M}{2}} w_l f_{i_1, i_2}(t'_l, s_{i_1, i_2}). \quad (43b)$$

Let s_{i_1, i_2}^* be the optimum value of s_{i_1, i_2} for the optimization problem in (43a). Then,

$$\begin{aligned} & \lim_{L \rightarrow \infty} \max_{t_1, t_2, \dots, t_L} \min_{\substack{i_1, i_2 \in \{0, \dots, M-1\}, \\ i_1 \neq i_2}} \max_{s_{i_1, i_2}} \frac{1}{L} \sum_{l=1}^L f_{i_1, i_2}(t_l, s_{i_1, i_2}) \\ & \geq \lim_{L \rightarrow \infty} \max_{t_1, t_2, \dots, t_L} \min_{\substack{i_1, i_2 \in \{0, \dots, M-1\}, \\ i_1 \neq i_2}} \frac{1}{L} \sum_{l=1}^L f_{i_1, i_2}(t_l, s_{i_1, i_2}^*) \\ & \stackrel{(a)}{=} \max_{w_1, w_2, \dots, w_{\binom{M}{2}}} \max_{t'_1, t'_2, \dots, t'_{\binom{M}{2}}} \min_{\substack{i_1, i_2 \in \{0, \dots, M-1\}, \\ i_1 \neq i_2}} w_l f_{i_1, i_2}(t'_l, s_{i_1, i_2}^*) = \\ & = \max_{w_1, w_2, \dots, w_{\binom{M}{2}}} \max_{t'_1, t'_2, \dots, t'_{\binom{M}{2}}} \min_{\substack{i_1, i_2 \in \{0, \dots, M-1\}, \\ i_1 \neq i_2}} \max_{s_{i_1, i_2}} \sum_{l=1}^{\binom{M}{2}} w_l f_{i_1, i_2}(t'_l, s_{i_1, i_2}), \end{aligned} \quad (44)$$

where (a) follows from (41). If s_{i_1, i_2}^{**} is the optimum value of s_{i_1, i_2} for the optimization problem in (43b),

$$\begin{aligned} & \max_{w_1, w_2, \dots, w_{\binom{M}{2}}} \max_{t'_1, t'_2, \dots, t'_{\binom{M}{2}}} \min_{\substack{i_1, i_2 \in \{0, \dots, M-1\}, \\ i_1 \neq i_2}} \max_{s_{i_1, i_2}} \sum_{l=1}^{\binom{M}{2}} w_l f_{i_1, i_2}(t'_l, s_{i_1, i_2}) \\ & \geq \max_{w_1, w_2, \dots, w_{\binom{M}{2}}} \max_{t'_1, t'_2, \dots, t'_{\binom{M}{2}}} \min_{\substack{i_1, i_2 \in \{0, \dots, M-1\}, \\ i_1 \neq i_2}} \sum_{l=1}^{\binom{M}{2}} w_l f_{i_1, i_2}(t'_l, s_{i_1, i_2}^{**}) \\ & \stackrel{(b)}{=} \lim_{L \rightarrow \infty} \max_{t_1, t_2, \dots, t_L} \min_{\substack{i_1, i_2 \in \{0, \dots, M-1\}, \\ i_1 \neq i_2}} \frac{1}{L} \sum_{l=1}^L f_{i_1, i_2}(t_l, s_{i_1, i_2}^{**}) \\ & = \lim_{L \rightarrow \infty} \max_{t_1, t_2, \dots, t_L} \min_{\substack{i_1, i_2 \in \{0, \dots, M-1\}, \\ i_1 \neq i_2}} \max_{s_{i_1, i_2}} \frac{1}{L} \sum_{l=1}^L f_{i_1, i_2}(t_l, s_{i_1, i_2}), \end{aligned} \quad (45)$$

where (b) follows from (41). Hence, using (44) and (45), we obtain (43). \square

Remark 1. From the above lemma, for binary hypothesis, i.e., $M = 2$, it can be easily seen that the sub-optimum sampling times when $L \rightarrow \infty$ are the same ($t_{1,CI} = \dots = t_{L,CI}$) and equal to the sampling

time when $L = 1$. This result is also true for the limited values of L which is shown in Lemma 7.¹

Lemma 6. (Sub-optimum sampling time using Gaussian approximation when $M = 2$) For binary hypothesis, the sub-optimum values of the sampling times t_1, t_2, \dots, t_L using Gaussian approximation are the solutions of:

$$\begin{aligned} & \frac{1}{\sigma_0} \exp\left(\frac{-(\beta - \mu_0)^2}{2\sigma_0^2}\right) \left[g_{0,l} - g_{1,l} - \left(\frac{g_{0,l}}{\lambda_{0,l}} - \frac{g_{1,l}}{\lambda_{1,l}}\right) \lambda_{0,l} \left(1 + \frac{1}{\sigma_0^2}\right) - w_l g_{0,l} \left(1 + \frac{1}{2\sigma_0^2}\right) \right] \\ & - \frac{1}{\sigma_1} \exp\left(\frac{-(\beta - \mu_1)^2}{2\sigma_1^2}\right) \left[g_{0,l} - g_{1,l} - \left(\frac{g_{0,l}}{\lambda_{0,l}} - \frac{g_{1,l}}{\lambda_{1,l}}\right) \lambda_{1,l} \left(1 + \frac{1}{\sigma_1^2}\right) - w_l g_{1,l} \left(1 + \frac{1}{2\sigma_1^2}\right) \right] = 0, \end{aligned} \quad (46)$$

for $l = 1, \dots, L$, where $\mu_i = \sum_{l=1}^L w_l \lambda_{i,l}$, $\sigma_i = \sqrt{\sum_{l=1}^L w_l^2 \lambda_{i,l}}$, $g_{i,l} = \frac{d}{dt} \lambda_{i,l}$, $i = 0, 1$, and β and w_l are defined in Corollary 2.1. For the location invariant flow velocity and the transparent receiver, we have $g_{i,l} = \lambda_{i,l} \left[\frac{-3}{2(t_l - t_r)} + \frac{\langle \mathbf{v}_i(t_l), \mathbf{r}_0 - \int_{t_r}^{t_l} \mathbf{v}_i(\tau) d\tau \rangle}{2D(t_l - t_r)} + \frac{\|\mathbf{r}_0 - \int_{t_r}^{t_l} \mathbf{v}_i(\tau) d\tau\|^2}{4D(t_l - t_r)^2} \right]$, $i = 0, 1$.

Proof. The proof is provided in Appendix C. □

Lemma 7. (Sub-optimum sampling times using CI upper bound when $M = 2$) The sub-optimum values of the sampling times for binary hypothesis and L sample receiver using CI upper bound are the same and equal to the sampling time of $L = 1$, noted by, t_1 , which is the solution of:

$$\begin{cases} g_{0,1}s + g_{1,1}(1-s) - s g_{0,1} \left(\frac{\lambda_{1,1}}{\lambda_{0,1}}\right)^{1-s} - (1-s) g_{1,1} \left(\frac{\lambda_{0,1}}{\lambda_{1,1}}\right)^s = 0, \\ s = \frac{\ln\left(\frac{\lambda_{0,1}}{\lambda_{1,1}} - 1\right) - \ln \ln\left(\frac{\lambda_{0,1}}{\lambda_{1,1}}\right)}{\ln\left(\frac{\lambda_{0,1}}{\lambda_{1,1}}\right)}, \end{cases} \quad (47)$$

where $g_{i,1}$ is defined in Lemma 6.

Proof. The proof is provided in Appendix D. □

IV. FLOW VELOCITY ESTIMATOR WITH L -SAMPLE RECEIVER

Here, we obtain the estimation of the flow velocity for the L -sample receiver with independent observations y_1, \dots, y_L in time instances t_1, \dots, t_L . We denote the mean number of the received molecules in sampling time t_l for the flow velocity \mathbf{v} as $\lambda_l(\mathbf{v})$, $l = 1, \dots, L$. For the transparent receiver, $\lambda_l(\mathbf{v}) =$

¹ Note that the problem of finding the optimum sampling times of the flow velocity detector can also be seen as either active hypothesis testing or channel discrimination problems, on which there are extensive literatures. In active hypothesis testing, the decision maker has control on the actions and the goal is to find the appropriate actions. In channel discrimination problem (with an extensive literature on quantum channels), there are a number of channels which we want to discriminate between and the inputs of the channels are chosen to have minimum error probability. The actions in active hypothesis testing and the inputs in channel discrimination problem are translated to sampling times in our model. For $M = 2$, in [37], [38], it is also shown that the actions that minimize CI upper bound are equal.

$V_R \zeta h_0(\mathbf{r}_0 - \mathbf{v} \cdot (t_l - t_r), t_l)$. We obtain the MAP and MMSE estimators for a randomly chosen constant flow velocity, i.e., $\mathbf{v}(\mathbf{r}, t) = \mathbf{v} = (v_x, v_y, v_z)$. We assume that v_x , v_y , and v_z are independent with prior probability distribution functions (PDF) as $p_x(v_x)$, $p_y(v_y)$, and $p_z(v_z)$, respectively. To investigate the error performance of the estimators, we consider the minimum mean square error (MSE) of the estimators and obtain the Bayesian Cramer-Rao (BCR) lower bound on the MSE of the estimators.

Lemma 8. (MAP estimator) *For a molecular flow velocity estimator to estimate randomly chosen constant flow velocity, the MAP estimator is obtained as*

$$\hat{\mathbf{v}} = \arg \max_{\mathbf{v}} \sum_{l=1}^L [y_l \ln(\lambda_l(\mathbf{v})) - \lambda_l(\mathbf{v})] + \ln(p_{x,y,z}(\mathbf{v})), \quad (48)$$

where, $p_{x,y,z}(\mathbf{v}) = p_x(v_x)p_y(v_y)p_z(v_z)$. Hence, if $p_{x,y,z}(\mathbf{v})$ and $\lambda_l(\mathbf{v})$ are differentiable with respect to \mathbf{v} , \hat{v}_x , \hat{v}_y , and \hat{v}_z are the solution of the following set of equations:

$$\sum_{l=1}^L \frac{1}{\lambda_l(\mathbf{v})} \cdot \frac{\partial \lambda_l(\mathbf{v})}{\partial v_i} \cdot (y_l - \lambda_l(\mathbf{v})) + \frac{1}{p_i(v_i)} \cdot \frac{dp_i(v_i)}{dv_i} = 0, \quad i \in \{x, y, z\}. \quad (49)$$

For the transparent receiver, we have $\frac{\partial \lambda_i(\mathbf{v})}{\partial v_i} = \frac{(\mathbf{r}_{0,i} - v_i \cdot (t_l - t_r))}{2D} \lambda_i(\mathbf{v})$, $i \in \{x, y, z\}$.

Proof. For the MAP estimator, we have

$$\hat{\mathbf{v}} = \arg \max_{\mathbf{v}} P(y_1, y_2, \dots, y_L | \mathbf{v}) P(\mathbf{v}), \quad (50)$$

which results in (48) for the independent observations. Let

$$R_{\text{est}}(\mathbf{v}) = \sum_{l=1}^L [y_l \ln(\lambda_l(\mathbf{v})) - \lambda_l(\mathbf{v})] + \ln(p_{x,y,z}(\mathbf{v})). \quad (51)$$

Hence, using $\frac{\partial R_{\text{est}}(\mathbf{v})}{\partial v_i} = 0$, it is straightforward to obtain (49). \square

Corollary 8.1. *For one-sample receiver and the location invariant flow velocity in the direction of the connecting line between the releasing node and the transparent receiver, i.e., $\mathbf{v} = v\mathbf{d}$, where $\mathbf{d} = \frac{\mathbf{r}_0}{r_0}$, with uniform priori PDF for v in the range $S_v = [v_{\min}, v_{\max}]$, the MAP estimator of v is obtained as*

$$\hat{v} = \begin{cases} v_1, & \text{if } y_1 \geq \lambda_1(v_1\mathbf{d}), v_1 \in S_v, \\ v_2, & \text{if } 0 < y_1 < \lambda_1(v_1\mathbf{d}), v_2 \in S_v, \\ v_3, & \text{if } 0 < y_1 < \lambda_1(v_1\mathbf{d}), v_3 \in S_v, \\ v_{\min}, & \text{if } (\{y_1 \geq \lambda_1(v_1\mathbf{d}), v_1 \notin S_v\} \cup \{0 < y_1 < \lambda_1(v_1\mathbf{d}), v_2 \notin S_v, v_3 \notin S_v\} \cup \{y_1 = 0\}) \cap B_1, \\ v_{\max}, & \text{if } (\{y_1 \geq \lambda_1(v_1\mathbf{d}), v_1 \notin S_v\} \cup \{0 < y_1 < \lambda_1(v_1\mathbf{d}), v_2 \notin S_v, v_3 \notin S_v\} \cup \{y_1 = 0\}) \cap B_2, \end{cases} \quad (52)$$

where $v_1 = \frac{r_0}{t_1 - t_r}$, $v_2 = \frac{r_0 + \sqrt{-4D(t_1 - t_r)(\ln y_l - \ln(\lambda_1(v_1 \mathbf{d}))})}{t_1 - t_r}$, $v_3 = \frac{r_0 - \sqrt{-4D(t_1 - t_r)(\ln y_l - \ln(\lambda_1(v_1 \mathbf{d}))})}{t_1 - t_r}$, $B_1 : \{R_{est,u}(v_{min}) \geq R_{est,u}(v_{max})\}$, and $B_2 : \{R_{est,u}(v_{min}) \leq R_{est,u}(v_{max})\}$, in which $R_{est,u}(v) = y_l \ln(\lambda_1(v \mathbf{d})) - \lambda_1(v \mathbf{d})$. Note that when the estimator gives two values, one of them is chosen randomly as the estimated value.

Proof. The proof is provided in Appendix E. \square

Corollary 8.2. *If the sampling times are equal, we have $\lambda_1(\mathbf{v}) = \dots = \lambda_L(\mathbf{v})$. Hence, from (49), we should find the solutions of*

$$\frac{1}{\lambda_l(\mathbf{v})} \frac{\partial \lambda_l(\mathbf{v})}{\partial v_i} \cdot \left(\sum_{l=1}^L y_l - L \lambda_l(\mathbf{v}) \right) + \frac{1}{p_i(v_i)} \frac{dp_i(v_i)}{dv_i} = 0, \quad i \in \{x, y, z\}, \quad (53)$$

to obtain the estimated values of v_x, v_y , and v_z . For the transparent receiver and the flow velocity in the direction of the releasing node and the receiver with uniform prior pdf for its magnitude, we should find the solution of $(r_0 - v \cdot (t_1 - t_r)) \cdot (\frac{1}{L} \sum_{l=1}^L y_l - \lambda_1(v \mathbf{d})) = 0$. Hence, the procedure to obtain the estimated value of v is similar to the one-sample receiver which is obtained in Corollary 8.1, with the difference that we should use $\frac{1}{L} \sum_{l=1}^L y_l$ instead of y_l in the equations, i.e., we should take the average of the samples and replace it as the observation value in the one-sample receiver.

Lemma 9. (MMSE estimator) *The MMSE estimator to estimate randomly chosen constant flow velocity with finite mean and variance is obtained as*

$$\hat{v}_i = \mathbb{E}[v_i | y_1, \dots, y_L] = \frac{\int v_i \exp(R_{est}(\mathbf{v})) dv_z dv_y dv_x}{\int \exp(R_{est}(\mathbf{v})) dv_z dv_y dv_x}, \quad i \in \{x, y, z\}, \quad (54)$$

where $R_{est}(\mathbf{v})$ is defined in (51). The linear MMSE (LMMSE) estimator is obtained as:

$$\hat{v}_i = \sum_{l=1}^L \frac{\text{Cov}(Y_l, v_i)}{\text{Var}(Y_l)} (y_l - \mathbb{E}[Y_l]) + \mathbb{E}[v_i], \quad (55)$$

for $i \in \{x, y, z\}$, where for $l = 1, \dots, L$,

$$\mathbb{E}[Y_l] = \int p_{x,y,z}(\mathbf{v}) \lambda_l(\mathbf{v}) dv_z dv_y dv_x, \quad (56)$$

$$\mathbb{E}[Y_l^2] = \int p_{x,y,z}(\mathbf{v}) \lambda_l(\mathbf{v}) (1 + \lambda_l(\mathbf{v})) dv_z dv_y dv_x,$$

$$\text{Cov}(Y_l, v_i) = \int p_{x,y,z}(\mathbf{v}) (v_i - \mathbb{E}[v_i]) \lambda_l(\mathbf{v}) dv_z dv_y dv_x, \quad i \in \{x, y, z\}.$$

Proof. The proof is provided in Appendix F. \square

Corollary 9.1. *For $\mathbf{v} = v \mathbf{d}$, with uniform prior PDF for v in range $S_v = [v_{min}, v_{max}]$, the MMSE estimator is obtained as*

$$\hat{v} = \frac{\int_{S_v} v \exp(\sum_{l=1}^L [y_l \ln(\lambda_l(v \mathbf{d})) - \lambda_l(v \mathbf{d})]) dv}{\int_{S_v} \exp(\sum_{l=1}^L [y_l \ln(\lambda_l(v \mathbf{d})) - \lambda_l(v \mathbf{d})]) dv}, \quad (57)$$

and the LMMSE estimator is obtained as

$$\hat{v} = \sum_{l=1}^L \frac{\text{Cov}(Y_l, v)}{\text{Var}(Y_l)} (y_l - \mathbb{E}[Y_l]) + \frac{v_+}{2}, \quad (58)$$

where for $l = 1, \dots, L$,

$$\begin{aligned} \mathbb{E}[Y_l] &= \frac{1}{v_-} \int_{S_v} \lambda_l(v\mathbf{d}) dv, & \mathbb{E}[Y_l^2] &= \frac{1}{v_-} \int_{S_v} \lambda_l(v\mathbf{d})(1 + \lambda_l(v\mathbf{d})) dv, \\ \text{Cov}(Y_l, v) &= \frac{1}{v_-} \int_{S_v} (v - \frac{v_+}{2}) \lambda_l(v\mathbf{d}) dv, \end{aligned} \quad (59)$$

where $v_+ = v_{\min} + v_{\max}$ and $v_- = v_{\max} - v_{\min}$.

Corollary 9.2. *If the sampling times are equal, the LMMSE estimator is obtained as*

$$\hat{v}_i = L \frac{\text{Cov}(v_i Y_1)}{\text{Var}(Y_1)} \left(\frac{1}{L} \sum_{l=1}^L y_l - \mathbb{E}[Y_1] \right) + \mathbb{E}[v_i], \quad i \in \{x, y, z\}. \quad (60)$$

In the following, we investigate the error performance of the estimators. The estimation error is $\epsilon = \mathbf{v} - \hat{\mathbf{v}}$, where ϵ_i is a random variable (v_i s are random variables with prior PDF $p_i(v_i)$ and \hat{v}_i is a function of Poisson random variables Y_1, \dots, Y_L). To investigate the performance of the estimators, we consider the MSE of the estimation, i.e., $\mathbb{E}[\epsilon^2]$ (where $\epsilon = \|\epsilon\|_2$), which is hard to compute in general case. In Section V, we obtain the MSE of the considered estimators numerically. In the following, we obtain the Bayesian and expected Cramer-Rao lower bounds on the MSE. The Bayesian Cramer-Rao (BCR) lower bound on the MSE is defined as [39]

$$\mathbb{E}[\epsilon^2] \geq \text{Tr}\{J_B^{-1}\}, \quad J_B = -\mathbb{E}_{\mathbf{v}, \mathbf{Y}}[\nabla_{\mathbf{v}\mathbf{v}}^2(\ln(\mathbb{P}(\mathbf{v}, \mathbf{y})))] \quad (61)$$

where $\mathbf{Y} = (Y_1, \dots, Y_L)$. J_B can be divided into two matrixes J_P and J_D :

$$J_B = J_D + J_P, \quad J_D = \mathbb{E}_{\mathbf{v}}[J_F(\mathbf{v})], \quad J_P = -\mathbb{E}_{\mathbf{v}}[\nabla_{\mathbf{v}\mathbf{v}}^2(\ln(\mathbb{P}(\mathbf{v})))], \quad (62)$$

where

$$J_F(\mathbf{v}) = -\mathbb{E}_{\mathbf{Y}|\mathbf{v}}[\nabla_{\mathbf{v}\mathbf{v}}^2(\ln(\mathbb{P}(\mathbf{Y}|\mathbf{v})))] \quad (63)$$

is Fisher's information matrix. The following conditions must hold for the BCR lower bound:

- $\frac{\partial \ln(\mathbb{P}(\mathbf{v}, \mathbf{Y}))}{\partial v_i}$ and $\frac{\partial^2 \ln(\mathbb{P}(\mathbf{v}, \mathbf{Y}))}{\partial v_i \partial v_j}$, for $i, j \in \{x, y, z\}$, are absolutely integrable with respect to \mathbf{v} and \mathbf{Y} .
- $\lim_{v_i \rightarrow \pm\infty} b(\mathbf{v})\mathbb{P}(\mathbf{v}) = 0$, for $i \in \{x, y, z\}$, where $\mathbf{b}(\mathbf{v})$ is called the bias function defined as

$$\mathbf{b}(\mathbf{v}) = \mathbb{E}_{\mathbf{Y}|\mathbf{v}}[\hat{\mathbf{v}}] - \mathbf{v}. \quad (64)$$

The BCR lower bound is obtained in the following lemma.

Lemma 10. (BCR lower bound on MSE) *The BCR lower bound on the MSE to estimate randomly chosen constant flow velocity is obtained as*

$$\mathbb{E}[\epsilon^2] \geq \text{Tr}\{(J_D + J_P)^{-1}\}, \quad \{J_D\}_{i,j} = \sum_{l=1}^L \mathbb{E}_{\mathbf{v}} \left[\frac{1}{\lambda_l(\mathbf{v})} \cdot \frac{\partial \lambda_l(\mathbf{v})}{\partial v_i} \cdot \frac{\partial \lambda_l(\mathbf{v})}{\partial v_j} \right], \quad i, j \in \{x, y, z\}, \quad (65)$$

$$\{J_P\}_{i,j} = \begin{cases} -\sum_{l=1}^L \mathbb{E}_{v_i} \left[\frac{d^2 \ln(p_i(v_i))}{dv_i^2} \right], & i = j \\ 0, & i \neq j \end{cases}, \quad i, j \in \{x, y, z\}, \quad (66)$$

where the following conditions must hold:

- $\frac{\partial \ln(P(\mathbf{v}, \mathbf{Y}))}{\partial v_i}$ and $\frac{\partial^2 \ln(P(\mathbf{v}, \mathbf{Y}))}{\partial v_i \partial v_j}$ are absolutely integrable with respect to \mathbf{v} and \mathbf{Y} .
- $\lim_{v_i \rightarrow \pm\infty} b(\mathbf{v}) p_{x,y,z}(\mathbf{v}) = 0$, where $p_{x,y,z}(\mathbf{v})$ is defined in Lemma 8 and $b(\mathbf{v})$ is defined in (64).

Proof. The proof is provided in Appendix G. □

Although the BCR lower bound is valid for both biased and unbiased estimators, due to the conditions which must hold for the BCR lower bound, this lower bound is not valid when prior distribution is bounded (e.g., uniform distribution). Another lower bound on the MSE is the expected Cramer-Rao (ECR) lower bound, defined as [40]

$$\mathbb{E}[\epsilon^2] \geq \mathbb{E}_{\mathbf{v}} [\text{Tr}\{(1 + \mathbf{b}'(\mathbf{v})) J_F^{-1}(\mathbf{v})(1 + \mathbf{b}'(\mathbf{v}))^T + \|\mathbf{b}(\mathbf{v})\|^2\}], \quad (67)$$

where, $J_F(v)$ and $\mathbf{b}(v)$ are defined in (63). The following condition must hold for the ECR lower bound:

- $\frac{\partial \ln(P(\mathbf{Y}|\mathbf{v}))}{\partial v_i}$ and $\frac{\partial^2 \ln(P(\mathbf{Y}|\mathbf{v}))}{\partial v_i \partial v_j}$, for $i, j \in \{x, y, z\}$, are absolutely integrable.

Since there is no condition on the distribution of \mathbf{v} , the ECR lower bound is valid for all distributions over v including the bounded distributions. However, the bias function \mathbf{b} should be obtained for each estimator, which might be challenging. In [40], \mathbf{b} is optimized to obtain a general lower bound on all estimators. For $\mathbf{v} = v\mathbf{d}$, and bounded distributions for v , i.e, $v \in \{v_{\min}, v_{\max}\}$, the optimal bias function $b(v)$ is the solution of the following differential equation [40]:

$$J_F(v)b(v) = b''(v) + (1 + b'(v)) \left(\frac{d \ln P(v)}{dv} - \frac{d \ln(J_F(v))}{dv} \right), \quad (68)$$

within the range $v \in \{v_{\min}, v_{\max}\}$, with boundary condition $b'(v_{\min}) = b'(v_{\max}) = -1$. The ECR lower bound on the MSE is obtained in the following lemma for the transparent receiver and $\mathbf{v} = v\mathbf{d}$ with uniform distribution for $v \in \{v_{\min}, v_{\max}\}$.

Lemma 11. (ECR lower bound on MSE for uniform prior PDF) *For $L = 1$ and $\mathbf{v} = v\mathbf{d}$, with uniform prior PDF for v in range $S_v = [v_{\min}, v_{\max}]$, the ECR lower bound is obtained as*

$$\mathbb{E}[\epsilon^2] \geq \frac{1}{v_-} \int_{S_v} \left[\frac{(1 + b'(v))^2}{J_F(v)} + b^2(v) \right] dv, \quad (69)$$

where $J_F(v) = \frac{1}{4D^2}(r_0 - v.(t_l - t_r))^2\lambda_1(v\mathbf{d})$, v_- is defined in Corollary 9.1, and the optimal bias function $b(v)$ is the solution of the following ordinary differential equation:

$$J_F(v)b(v) = b''(v) - (1 + b'(v))\left(\frac{r_0 - v.(t_l - t_r)}{2D} - \frac{2(t_l - t_r)}{r_0 - v.(t_l - t_r)}\right), \quad (70)$$

for $v \in (v_{min}, v_{max})$, with condition $b'(v_{min}) = b'(v_{max}) = -1$.

Proof. The proof is straightforward from (67), (68). \square

Optimum and sub-optimum sampling times: To obtain the optimum sampling times, we minimize the MSE, for t_1, \dots, t_L , i.e.,

$$[t_1^*, t_2^* \dots t_L^*] = \arg \min_{t_1, t_2, \dots, t_L} E[\epsilon^2]. \quad (71)$$

However, the distribution of ϵ is hard to compute in general case. In Section V, we obtain the estimation error and the optimum sampling times numerically. In Lemma 12, when $L \rightarrow \infty$, we obtain the optimum sampling times for an MAP estimator of the magnitude of the flow velocity which is in the direction of the connecting line between the releasing node and the receiver with uniform distribution.

Lemma 12. (*Optimum sampling times for an MAP estimator when $L \rightarrow \infty$)* The optimum sampling times for an MAP estimator of $\mathbf{v} = v\mathbf{d}$, with uniform distribution for v , when $L \rightarrow \infty$ are at most two distinct times t_1 and t_2 with weights \tilde{w}_1 and \tilde{w}_2 , respectively, i.e., $L\tilde{w}_1$ sampling times are equal to t_1 and $L\tilde{w}_2$ sampling times are equal to t_2 . The two sampling times and their weights can be obtained from (71) numerically.

Proof. When $L \rightarrow \infty$, if the magnitude of the flow velocity is v_r , the average value of the observations $\frac{1}{L} \sum_{l=1}^L y_l$ approaches to $\lambda_1(v_r\mathbf{d})$. Hence, if the samples are taken at the same time, from (53), \hat{v} is the solution of $\frac{1}{L} \sum_{l=1}^L y_l - \lambda_1(v\mathbf{d}) = 0$, we obtain v_r and $v_r + \frac{2r_0}{(t_1 - t_r)}$ as the maximizers of $R_{\text{est}}(v\mathbf{d})$, which means that we may have ambiguity on the estimated flow velocity. This is because of the fact that the function $\lambda_l(v\mathbf{d})$ is not a one by one function of v . Since logarithm of the function $\lambda_l(v\mathbf{d})$ is a Quadratic function, using two values of $\lambda_l(v\mathbf{d})$, for two different sampling times, we can obtain v , i.e., if we have $\lambda_1(v\mathbf{d}) = a_1$ and $\lambda_2(v\mathbf{d}) = a_2$, we can obtain v uniquely. Note that the flow velocity is chosen randomly and for each flow velocity, every two different sampling times leads to a unique estimation. Hence, we conclude that when $L \rightarrow \infty$, if we have two different times, the estimation error approaches to zero. \square

V. SIMULATION AND NUMERICAL RESULTS

In this section, we provide some simulation and numerical results to evaluate the performance of the proposed flow velocity detector and estimator. For the evaluation, we use the parameters given in table I.

TABLE I: Simulation and numerical analysis parameters

Parameter	Value
D	$10^{-8} \text{ m}^2/\text{s}$
ζ	10000
r_0	100 μm
r_R	1.5×10^{-5}
t_r	0

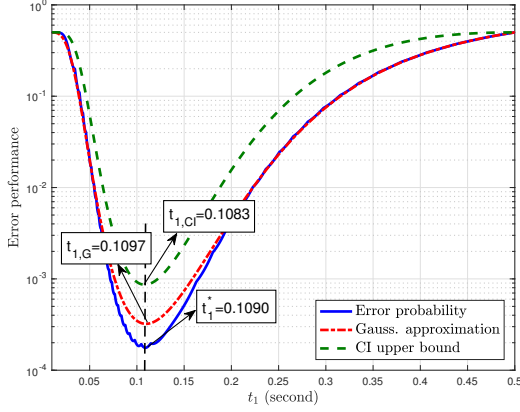
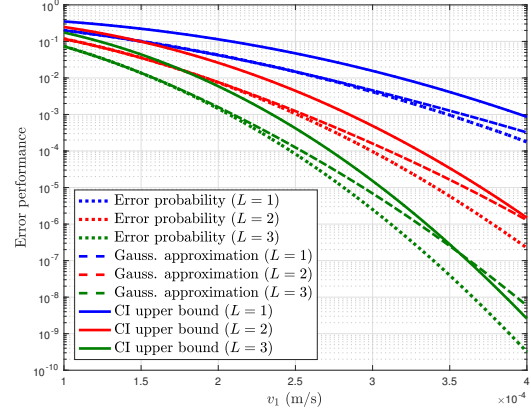
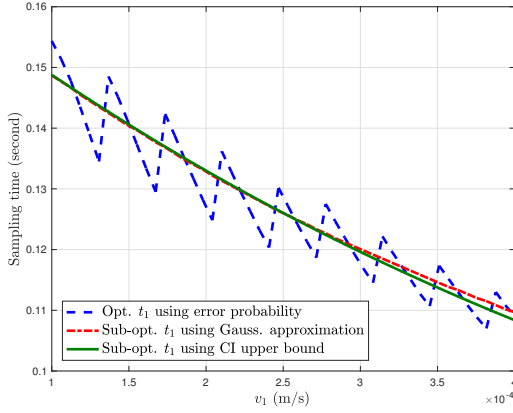
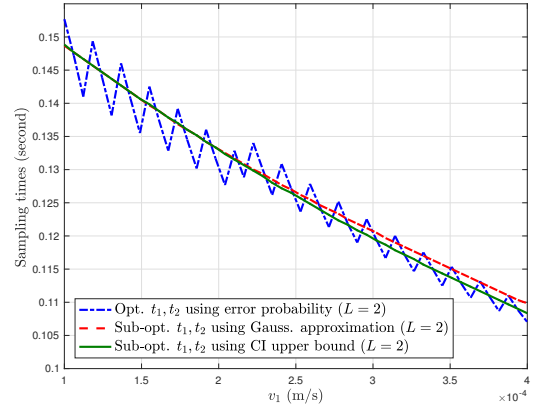
In part A, we consider the flow velocity detector, and in part B, we consider the flow velocity estimator. In both parts, we assume that the flow velocity is in the direction of the connecting line between the releasing node and the receiver.

A. Flow velocity detector

Here, we assume binary and multiple hypotheses for the flow velocity. We assume that the hypotheses in the flow velocity detector are location and time invariant, i.e., $\mathbf{v}_i(\mathbf{r}, t) = v_i \mathbf{d}, i \in \{0, 1, \dots, M - 1\}$.

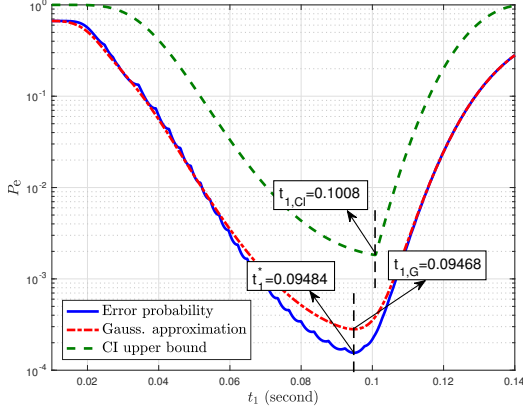
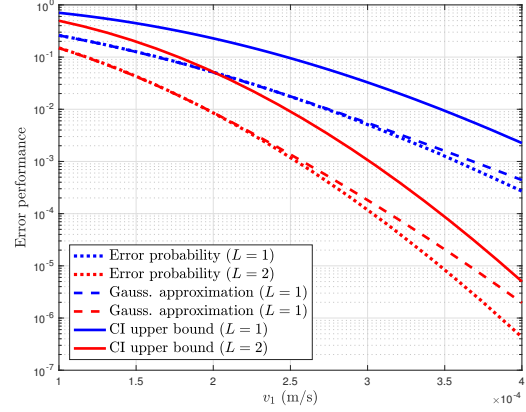
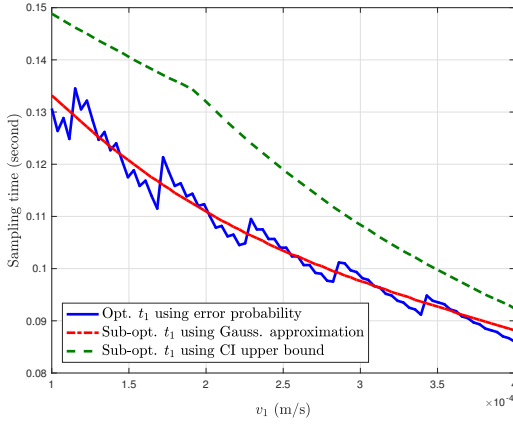
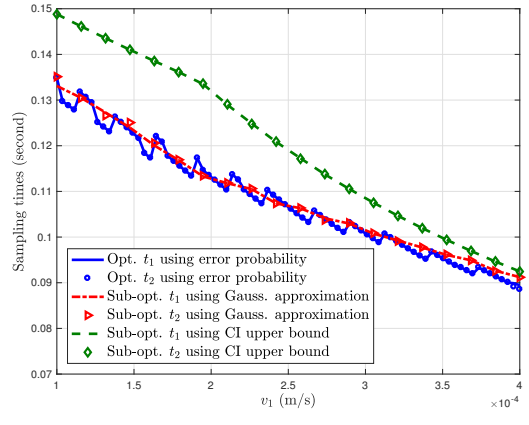
1) *Binary hypothesis* ($M = 2$): The error probability and its Gaussian approximation for binary hypothesis with one-sample decoder, derived in (23) and (24), respectively, and the CI upper bound, derived in (34), are depicted in Fig. 2a versus the sampling time t_1 for $v_0 = 0, v_1 = 4 \times 10^{-4} \text{ m/s}$. The sampling times, which minimize the error probability, and its Gaussian approximation and CI upper bound are $t_1^* = 0.1090 \text{ s}$, $t_{1,G} = 0.1097 \text{ s}$, and $t_{1,CI} = 0.1083 \text{ s}$, respectively. It is seen that optimum and sub-optimum sampling times are nearly the same. We assume $v_0 = 0$ and depict the error probability, its Gaussian approximation, and CI upper bound for $L = 1, 2, 3$ in Fig. 2b versus v_1 for their related optimum and sub-optimum sampling times. As expected, the error probability, the Gaussian approximation and the CI upper bound decrease as v_1 increases. Further, it is seen that the Gaussian approximation is nearly the same as the exact error probability. But, it makes distance as the error probability reduces. The CI upper bound and the error probability has a nearly constant gap in all values of v_1 . The error probabilities and their Gaussian approximation and CI upper bound for $L = 2, 3$ have the same behavior as $L = 1$ with the difference that they decrease as L increases.

The sub-optimum sampling times, using CI upper bound and Gaussian approximation, given in Lemmas 7 and 6, along with the optimum sampling time using the exact error probability, are depicted versus v_1 in Fig. 2c. It is seen that the sub-optimum sampling times are nearly the same, and decrease as v_1 increases and the optimum sampling time, which minimizes the error probability, fluctuates around the sub-optimum value (the fluctuation is small and because of the discrete nature of the Poisson distribution). In Fig. 2d,

(a) Error performance versus t_1 for $L = 1$.(b) Error performance versus v_1 for $L = 1, 2, 3$ with related optimum sampling times.(c) Sampling times versus v_1 for $L = 1$.(d) Sampling times versus v_1 for $L = 2$.Fig. 2: Error performance and sampling times for a flow velocity detector with $M = 2$.

the sampling times are depicted versus v_1 for a two-sample decoder. As mentioned in the previous section, the analytic results show that for L sample decoder, the sampling times which minimize the CI upper bound are the same, which is verified by simulations i.e., $t_{1,CI} = \dots = t_{L,CI}$. It is seen using simulations that the L sampling times which minimize the error probability and its Gaussian approximation are also equal, i.e., $t_1^* = \dots = t_L^*$ and $t_{1,G} = \dots = t_{L,G}$ for our simulation parameters. Further, it can be seen by comparing Fig. 2c and Fig. 2d that the optimum sampling times for $L = 1, 2$ are approximately equal.

2) *Multiple hypotheses ($M > 2$):* Here, we assume $M = 3$ hypotheses. The error probability, Gaussian approximation and CI upper bound versus the sampling time t_1 for $v_0 = 0$, $v_1 = 4 \times 10^{-4}$ m/s, and $v_2 = 8 \times 10^{-4}$ m/s are depicted Fig. 3a. The sampling times that minimize the error probability, its Gaussian approximation and CI upper bound are obtained as $t_1^* = 0.09484$ s, $t_{1,G} = 0.09468$ s, and $t_{1,CI} = 0.1008$ s, respectively. It is seen that the CI upper bound has a gap with the error probability in

(a) Error performance versus t_1 for $L = 1$.(b) Error performance versus v_1 for $L = 1, 2, 3$ with related optimum sampling times.(c) Sampling times versus v_1 for $L = 1$.(d) Sampling times versus v_1 for $L = 2$.Fig. 3: Error performance and sampling times for a flow velocity detector with $M = 3$.

all values despite the binary case due to using union bound in multiple hypotheses case. The optimum value and the sub-optimum values of the sampling times are nearly equal. However, the sub-optimum value using CI upper bound has made a small gap from the optimum value compared to binary case, which may be due to the union bound. The error probability, the Gaussian approximation and the CI upper bound versus v_1 for the sampling times which minimize them are provided in Fig. 3b for $L = 1, 2$. It is seen that as expected, the error probability, Gaussian approximation, and CI upper bound decrease as L increases.

The sampling times which minimize the error probability, the Gaussian approximation, and the CI upper bound are depicted in Fig. 3c versus v_1 (we assumed $v_0 = 0, v_2 = 2v_1$ and changed v_1). As seen in this figure, the optimum value of the sampling time fluctuates around the sub-optimum value using Gaussian approximation. But the sub-optimum value using CI upper bound has a distance from these values, which

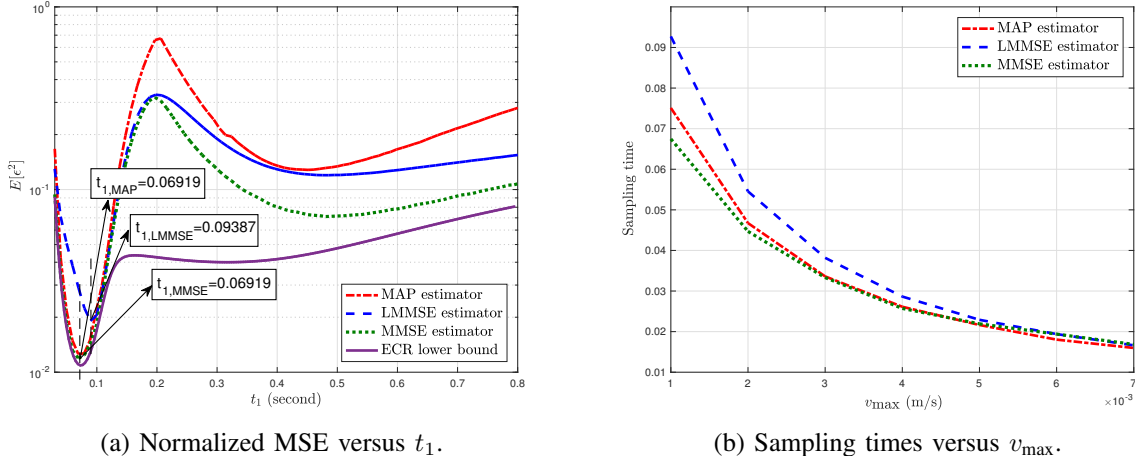


Fig. 4: Normalized MSE and sampling times for a flow velocity estimator with $M = 2$ and $L = 1$.

decreases as v_1 increases. For $L = 2$, we depict the two sampling times t_1 and t_2 versus v_1 in Fig. 3d. It is seen that similar to the binary case, the sampling times t_1 and t_2 which minimize the error probability, the Gaussian approximation, and the CI upper bound are equal, i.e., $t_1^* = t_2^*$, $t_{1,G} = t_{2,G}$, and $t_{1,CI} = t_{2,CI}$. Further, the optimum and sub-optimum sampling times are nearly the same as the values of the optimum and sub-optimum sampling times in one sample decoder.

For a large value of L (e.g., $L = 50$), we obtain the sub-optimum sampling times which minimize the CI upper bound using the optimization problem in (38). We assume $v_0 = 0$, $v_1 = 10^{-4}$ m/s, and $v_2 = 2 \times 10^{-4}$ m/s. Using (38), we obtain the $L = 50$ sampling times as $t_1 \approx \dots \approx t_{50} \approx 0.1488$ s. This is also confirmed by the results of Lemma 5 (which can be obtained from (39) equal to $t_{1,\text{Chernoff}} = t_{2,\text{Chernoff}} = t_{3,\text{Chernoff}} = 0.1488$ s). Note that Lemma 5 anticipates that the sub-optimum sampling times are *at most* $\binom{M}{2}$ different times. This is somehow counter-intuitive since we obtain a single distinct sampling time, while we expect to obtain three different sampling times. For some other simulation parameters, the same result, i.e., a single sampling time, is observed. Another approach to find the three sampling times that Lemma 5 anticipates is to obtain the optimum times that discriminate between $\{H_0, H_1\}$, $\{H_1, H_2\}$, and $\{H_0, H_2\}$ by using one-sample decoder and minimizing the CI upper bound. For $\{H_0, H_1\}$, we get $t_1 = 0.1488$ s, for $\{H_1, H_2\}$, we get $t_2 = 0.1231$ s, and for $\{H_0, H_2\}$, we get $t_3 = 0.1330$ s. Then, we use these sampling times in the optimization problem in Lemma 5 and obtain the three weights as $w_1^* = 1$, $w_2^* = 0$, $w_3^* = 0$, which matches the results obtained from (38) and Lemma 5.

B. Flow velocity estimator

Here, we assume that the magnitude of v has uniform distribution in the range $[v_{\min}, v_{\max}]$. The MSE of estimation, $E[\epsilon^2]$, normalized to $E[v]^2$, versus the sampling time is depicted in Fig. 4a for the MAP,

MMSE, and LMMSE estimators along with the ECR lower bound given in Lemma 11. We assume $v_{\min} = 0, v_{\max} = 1 \times 10^{-3}$ m/s. As expected the MMSE estimator has the least MSE. However, the LMMSE does not always have better performance than MAP, which is because of the force of linearity to the estimated value in LMMSE. Further, it is seen that the performance of the MAP estimator is near the MMSE estimator and the ECR lower bound around the optimum sampling time. Using this figure, the sampling times which minimize $E[\epsilon^2]$ for the MAP, MMSE, and LMMSE estimators are obtained as $t_{1,\text{MAP}} = 0.06919$ s, $t_{1,\text{MMSE}} = 0.06919$ s, and $t_{1,\text{LMMSE}} = 0.09387$ s, respectively. It is seen that the optimum sampling times of the MAP and MMSE are nearly the same. However, the optimum sampling time of the LMMSE has a small gap from these values. We assume $v_{\min} = 0$ and depict the optimum sampling times which minimize the MSE of the MAP, MMSE, and LMMSE estimators versus v_{\max} in Fig. 4b. It is seen that the optimum sampling times reduce as v_{\max} increases.

VI. CONCLUDING REMARKS AND FUTURE WORKS

In this paper, we designed a molecular flow velocity meter which consists of a molecule releasing node and a molecular receiver to detect the medium flow velocity. We first assumed M hypotheses for the medium flow velocity and a L -sample decoder at the receiver and obtained the optimum maximum-a-posteriori (MAP). We derived the error probability, its Gaussian approximation, and CI upper bound to analyze the performance of the detector. Further, we obtained the optimum and sub-optimum sampling times using the error probability, its Gaussian approximation, and CI upper bound. When $L \rightarrow \infty$, we obtained an interesting result using the CI upper bound which shows that for M hypotheses, the sub-optimum sampling times yields to $\binom{M}{2}$ sampling times $t_1, t_2, \dots, t_{\binom{M}{2}}$ with $\binom{M}{2}$ weights $w_1, w_2, \dots, w_{\binom{M}{2}}$, i.e., Lw_l sampling times are equal to t_l . For the simulation parameters, it is seen that these sampling times are the sampling times which minimize the CI upper bound for discriminating each two hypotheses. This results in a much simpler optimization problem to obtain the sub-optimum sampling times. Then, we assumed randomly chosen constant flow velocity in the medium and obtained the MAP and MMSE estimators for the L -sample receiver. We considered the mean square error (MSE) of the estimators and obtained the Bayesian Cramer-Rao (BCR) and expected Cramer-Rao (ECR) lower bounds on the MSE. We obtained the sampling times which minimize the MSE numerically. We showed that when $L \rightarrow \infty$, for the MAP estimator, two different sampling times are enough for estimation, i.e., $L\tilde{w}_1$ sampling times are t_1 and $L\tilde{w}_2$ sampling times are t_2 . The molecular flow velocity meter can have applications in health care to monitor the function of the heart. It can also be used to design a new modulation scheme in MC, in which information is encoded in the medium flow velocity, i.e., similar to the classic communications

that medium-based communication is introduced, we can introduce flow-based communication in MC. This makes the transmitter much simpler which is an important challenge in MC.

REFERENCES

- [1] S. R. Sakthivel, K. Sudarshanand, and V. Balaji Venkateswaran, "A survey on flow meters based on application," *International Journal of Engineering and Technology*, vol. 7, no. 2.6, pp. 206–212, 2018.
- [2] F. Yusheng, Q. Wang, J. Yi, D. Song, and X. Xiang, "A numerical model of blood flow velocity measurement based on finger ring," *Journal of healthcare engineering*, vol. 2018, 2018.
- [3] N. A. Lassen, O. Henriksen, and P. Sejrsen, "Indicator methods for measurement of organ and tissue blood flow," *Comprehensive physiology*, pp. 21–63, 2011.
- [4] S. Puri, J.-K. Park, F. Modersitzki, and D. S. Goldfarb, "Radioisotope blood volume measurement in hemodialysis patients," *Hemodialysis International*, vol. 18, no. 2, pp. 406–414, 2014.
- [5] K. Zierler, "Indicator dilution methods for measuring blood flow, volume, and other properties of biological systems: a brief history and memoir," *Annals of biomedical engineering*, vol. 28, no. 8, pp. 836–848, 2000.
- [6] L. Grote, D. Zou, H. Kraiczi, and J. Hedner, "Finger plethysmographya method for monitoring finger blood flow during sleep disordered breathing," *Respiratory physiology & neurobiology*, vol. 136, no. 2-3, pp. 141–152, 2003.
- [7] L. Blendis, V. Roberts, M. Spiro, and R. Williams, "The comparative measurement of splenic blood flow using 133xenon and an electromagnetic flowmeter," *Cardiovascular research*, vol. 4, no. 1, pp. 44–49, 1970.
- [8] W. Li and A. Ahn, "Effect of acupuncture manipulations at li4 or li11 on blood flow and skin temperature," *Journal of acupuncture and meridian studies*, vol. 9, no. 3, pp. 128–133, 2016.
- [9] C. T. Chou, "Extended master equation models for molecular communication networks," *IEEE Transactions on Nanobiotechnology*, vol. 12, no. 2, pp. 79–92, 2013.
- [10] A. Einolghozati, M. Sardari, and F. Fekri, "Design and analysis of wireless communication systems using diffusion-based molecular communication among bacteria," *IEEE Transactions on Wireless Communications*, vol. 59, pp. 6096–6105, December 2013.
- [11] S. Kadloor, R. Adve, and A. Eckford, "Molecular communication using brownian motion with drift," *IEEE Transactions on NanoBioscience*, vol. 11, pp. 89–99, June 2012.
- [12] H. Arjmandi, A. Gohari, M. Nasiri-Kenari, and F. Bateni, "Diffusion based nanonetworking: A new modulation technique and performance analysis," *IEEE Communication Letters*, vol. 17, no. 4, pp. 645–648, 2013.
- [13] G. Aminian, M. Farahnak-Ghazani, M. Mirmohseni, M. Nasiri-Kenari, and F. Fekri, "On the capacity of point-to-point and multiple-access molecular communications with ligand-receptors," *IEEE Transactions on Molecular, Biological and Multi-Scale Communications*, vol. 1, no. 4, pp. 331–346, 2016.
- [14] A. Einolghozati, M. Sardari, and F. Fekri, "Capacity of diffusion-based molecular communication with ligand receptors," in *Information Theory Workshop (ITW), 2011 IEEE*, pp. 85–89, IEEE, 2011.
- [15] H. Arjmandi, G. Aminian, A. Gohari, M. Nasiri-Kenari, and U. Mitra, "Capacity of diffusion based molecular communication networks over lti-poisson channels," *IEEE Transactions on Molecular, Biological and Multi-Scale Communications*, vol. 1, no. 2, pp. 188–201, 2014.
- [16] M. S. Leeson and M. D. Higgins, "Forward error correction for molecular communications," *Nano Communication Networks*, vol. 3, no. 3, pp. 161–167, 2012.
- [17] M. Mahfuz, D. Makrakis, and H. Mouftah, "Performance analysis of convolutional coding techniques in diffusion-based concentration-encoded pam molecular communication systems," *BioNanoScience*, vol. 3, no. 3, pp. 270–284, 2013.

- [18] R. Mosayebi, A. Gohari, M. Mirmohseni, and M. Nasiri-Kenari, "Type based sign modulation for molecular communication," in *Iran Workshop on Communication and Information Theory (IWCIT)*, May 2016.
- [19] M. Farahnak-Ghazani, G. Aminian, M. Mirmohseni, A. Gohari, and M. Nasiri-Kenari, "Physical layer network coding in molecular two-way relay networks," in *2016 Iran Workshop on Communication and Information Theory (IWCIT)*, pp. 1–6, May 2016.
- [20] A. Noel, K. C. Cheung, and R. Schober, "Improving receiver performance of diffusive molecular communication with enzymes," *NanoBioscience, IEEE Transactions on*, vol. 13, no. 1, pp. 31–43, 2014.
- [21] Y. Cho, B. Yilmaz, W. Guo, and C.-B. Chae, "Effective enzyme deployment for degradation of interference molecules in molecular communication," in *IEEE WCNC 2017 Conference Proceedings*, IEEE, 2017.
- [22] R. Mosayebi, H. Arjmandi, A. Gohari, M. Nasiri-Kenari, and U. Mitra, "Receivers for diffusion-based molecular communication: Exploiting memory and sampling rate," *IEEE Journal on Selected Areas in Communications*, vol. 32, no. 12, pp. 2368 – 2380, 2014.
- [23] M. Movahednasab, M. Soleimanifar, A. Gohari, M. Nasiri-Kenari, and U. Mitra, "Adaptive transmission rate with a fixed threshold decoder for diffusion-based molecular communication," *IEEE Transactions on Communications*, vol. 64, no. 1, pp. 236 – 248, 2015.
- [24] M. Farahnak-Ghazani, G. Aminian, M. Mirmohseni, A. Gohari, and M. Nasiri-Kenari, "On medium chemical reaction in diffusion-based molecular communication: A two-way relaying example," *IEEE Transactions on Communications*, vol. 67, no. 2, pp. 1117–1132, 2018.
- [25] V. Jamali, A. Ahmadzadeh, C. Jardin, H. Sticht, and R. Schober, "Channel estimation for diffusive molecular communications," *IEEE Transactions on Communications*, vol. 64, no. 10, pp. 4238–4252, 2016.
- [26] A. Noel, K. C. Cheung, and R. Schober, "Joint channel parameter estimation via diffusive molecular communication," *IEEE Transactions on Molecular, Biological and Multi-Scale Communications*, vol. 1, no. 1, pp. 4–17, 2015.
- [27] S. M. Rouzegar and U. Spagnolini, "Channel estimation for diffusive mimo molecular communications," in *2017 European Conference on Networks and Communications (EuCNC)*, pp. 1–5, IEEE, 2017.
- [28] H. V. Poor, *An introduction to signal detection and estimation*. Springer Science & Business Media, 2013.
- [29] A. Gohari, M. Mirmohseni, and M. Nasiri-Kenari, "Information theory of molecular communication: Directions and challenges," *IEEE Transactions on Molecular, Biological and Multi-Scale Communications*, 2016.
- [30] A. Noel, K. C. Cheung, and R. Schober, "Optimal receiver design for diffusive molecular communication with flow and additive noise," *IEEE transactions on nanobioscience*, vol. 13, no. 3, pp. 350–362, 2014.
- [31] T. Koike-Akino, J. Suzuki, and P. V. Orlik, "Molecular signaling design exploiting cyclostationary drift-diffusion fluid," in *IEEE Global Communications Conference (GLOBECOM)*, DEC. 2017.
- [32] N. Farsad, B. Yilmaz, A. Eckford, C.-B. Chae, and W. Guo, "A comprehensive survey of recent advancements in molecular communication," *IEEE Communications Surveys and Tutorials*, vol. 18, no. 1, pp. 1887 – 1919, 2016.
- [33] H. Chernoff, "A measure of asymptotic efficiency for tests of a hypothesis based on the sum of observations," *The Annals of Mathematical Statistics*, vol. 23, no. 4, pp. 493 – 507, 1952.
- [34] F. Nielsen, "Chernoff information of exponential families," *arXiv preprint arXiv:1102.2684*, 2011.
- [35] E. Beckenbach, "On hölder's inequality," *Journal of Mathematical Analysis and Applications*, vol. 15, no. 1, pp. 21–29, 1966.
- [36] R. Vershynin, *High-Dimensional Probability*. University of Michigan, 2017.
- [37] M. Hayashi, "Discrimination of two channels by adaptive methods and its application to quantum system," *IEEE Transactions on Information Theory*, vol. 55, no. 8, pp. 3807–3820, 2009.

- [38] S. Nitinawarat, G. K. Atia, and V. V. Veeravalli, "Controlled sensing for multihypothesis testing," *IEEE Transactions on Automatic Control*, vol. 58, no. 10, pp. 2451–2464, 2013.
- [39] H. L. Van Trees, *Detection, estimation, and modulation theory, part I: detection, estimation, and linear modulation theory*. John Wiley & Sons, 2004.
- [40] Z. Ben-Haim and Y. C. Eldar, "A lower bound on the bayesian mse based on the optimal bias function," *IEEE Transactions on Information Theory*, vol. 55, no. 11, pp. 5179–5196, 2009.

APPENDIX A

PROOF OF COROLLARY 3.1

For binary hypothesis, (18) is simplified as

$$P_e = 1 - \frac{1}{2} \left[\sum_{\substack{y_1, \dots, y_L=0, \\ \sum_{l=1}^L w_{0,1,l} y_l > \beta_{0,1}}} \prod_{l=1}^L \frac{(\lambda_{0,l})^{y_l} \exp(-\lambda_{0,l})}{y_l!} + \sum_{\substack{y_1, \dots, y_L=0, \\ \sum_{l=1}^L w_{1,0,l} y_l > \beta_{1,0}}} \prod_{l=1}^L \frac{(\lambda_{1,l})^{y_l} \exp(-\lambda_{1,l})}{y_l!} \right] \quad (72)$$

For this case, we have $w_{0,1,l} = -w_{1,0,l} = w_L$ and $\beta_{0,1} = -\beta_{1,0} = \beta$. Hence,

$$P_e = \frac{1}{2} \left[1 - \sum_{\substack{y_1, \dots, y_L=0, \\ \sum_{l=1}^L w_l y_l > \beta}} \prod_{l=1}^L \frac{(\lambda_{0,l})^{y_l} \exp(-\lambda_{0,l})}{y_l!} + \sum_{\substack{y_1, \dots, y_L=0, \\ \sum_{l=1}^L w_l y_l > \beta}} \prod_{l=1}^L \frac{(\lambda_{1,l})^{y_l} \exp(-\lambda_{1,l})}{y_l!} \right], \quad (73)$$

which reduces to (21). For the Gaussian approximation, we have

$$P_e = \frac{1}{2} \sum_{i=0}^{M-1} \left[1 - \text{P} \left\{ \sum_{l=1}^L w_l Y_l > \beta | H_0 \right\} + \text{P} \left\{ \sum_{l=1}^L w_l Y_l > \beta | H_1 \right\} \right]. \quad (74)$$

Since Y_l s are independent Gaussian variables, $Y = \sum_{l=1}^L w_l Y_l$ is a Gaussian variable with mean $\text{E}[Y] = \sum_{l=1}^L w_l \lambda_{i,l}$ and variance $\text{Var}(Y) = \sum_{l=1}^L w_l^2 \lambda_{i,l}$, for H_i . Hence, (74) reduces to (22).

APPENDIX B

PROOF OF COROLLARY 4.1

From holder's inequality, for any positive vectors $\mathbf{x} = (x_1, x_2, \dots, x_n)$ and $\mathbf{y} = (y_1, y_2, \dots, y_n)$ and for any p, q , satisfying $p > 1$ and $\frac{1}{p} + \frac{1}{q} = 1$, we have $(\sum_{i=1}^n x_i^p)^{\frac{1}{p}} (\sum_{i=1}^n y_i^q)^{\frac{1}{q}} \geq \sum_{i=1}^n x_i y_i$. Using this inequality for $\mathbf{x} = (\lambda_{i_1,1}^{s_{i_1,i_2}}, \dots, \lambda_{i_1,L}^{s_{i_1,i_2}})$, $\mathbf{y} = (\lambda_{i_2,1}^{1-s_{i_1,i_2}}, \dots, \lambda_{i_2,L}^{1-s_{i_1,i_2}})$, $p = \frac{1}{s_{i_1,i_2}}$, and $q = \frac{1}{1-s_{i_1,i_2}}$, we have:

$$\sum_{l=1}^L \lambda_{i_1,l}^{s_{i_1,i_2}} \lambda_{i_2,l}^{1-s_{i_1,i_2}} \leq \left(\sum_{l=1}^L \lambda_{i_1,l} \right)^{s_{i_1,i_2}} \left(\sum_{l=1}^L \lambda_{i_2,l} \right)^{1-s_{i_1,i_2}}. \quad (75)$$

Hence, we bound $D_{i_1,i_2}(s_{i_1,i_2})$ in (26) as follows:

$$D_{i_1,i_2}(s_{i_1,i_2}) \geq \left(\sum_{l=1}^L \lambda_{i_1,l} \right)^{s_{i_1,i_2}} + \left(\sum_{l=1}^L \lambda_{i_2,l} \right) (1 - s_{i_1,i_2}) - \left(\sum_{l=1}^L \lambda_{i_1,l} \right)^{s_{i_1,i_2}} \left(\sum_{l=1}^L \lambda_{i_2,l} \right)^{1-s_{i_1,i_2}} \quad (76)$$

Let $K_{i_1, i_2}(s_{i_1, i_2}) = (\sum_{l=1}^L \lambda_{i_1, l})s_{i_1, i_2} + (\sum_{l=1}^L \lambda_{i_2, l})(1 - s_{i_1, i_2}) - (\sum_{l=1}^L \lambda_{i_1, l})^{s_{i_1, i_2}} (\sum_{l=1}^L \lambda_{i_2, l})^{1-s_{i_1, i_2}}$. Then, (26) reduces to (30). Now using this bound, the optimum value of s_{i_1, i_2} is obtained by maximizing $K_{i_1, i_2}(s_{i_1, i_2})$ as the solution of the following equation:

$$\begin{aligned} \frac{d}{ds_{i_1, i_2}} K_{i_1, i_2}(s_{i_1, i_2}) &= \sum_{l=1}^L \lambda_{i_1, l} - \sum_{l=1}^L \lambda_{i_2, l} - \ln\left(\sum_{l=1}^L \lambda_{i_1, l}\right) \left(\sum_{l=1}^L \lambda_{i_1, l}\right)^{s_{i_1, i_2}} \left(\sum_{l=1}^L \lambda_{i_2, l}\right)^{1-s_{i_1, i_2}} \\ &\quad + \ln\left(\sum_{l=1}^L \lambda_{i_2, l}\right) \left(\sum_{l=1}^L \lambda_{i_1, l}\right)^{s_{i_1, i_2}} \left(\sum_{l=1}^L \lambda_{i_2, l}\right)^{1-s_{i_1, i_2}} = 0, \end{aligned} \quad (77)$$

which reduces to

$$s_{i_1, i_2} \ln\left(\frac{\sum_{l=1}^L \lambda_{i_1, l}}{\sum_{l=1}^L \lambda_{i_2, l}}\right) + \ln\ln\left(\frac{\sum_{l=1}^L \lambda_{i_1, l}}{\sum_{l=1}^L \lambda_{i_2, l}}\right) = \ln\left(\frac{\sum_{l=1}^L \lambda_{i_1, l}}{\sum_{l=1}^L \lambda_{i_2, l}} - 1\right). \quad (78)$$

Hence, s_{i_1, i_2}^* is obtained as (31).

APPENDIX C

PROOF OF LEMMA 6

From (37), we should solve the following optimization problem:

$$\max_{t_1, \dots, t_L} P_{e,G}, \quad (79)$$

where $P_{e,G}$ is given in (22). Hence, the sub-optimum values of t_1, \dots, t_L are the solutions of $\nabla P_{e,G} = [\frac{\partial P_{e,G}}{\partial t_1}, \dots, \frac{\partial P_{e,G}}{\partial t_L}] = 0$. Let $\mu_i = \sum_{l=1}^L w_l \lambda_{i,l}$ and $\sigma_i = \sqrt{\sum_{l=1}^L w_l^2 \lambda_{i,l}}$ in (22). Hence, from $\frac{\partial P_{e,G}}{\partial t_i} = 0$, we obtain:

$$\begin{aligned} \exp\left(\frac{-(\beta - \mu_0)^2}{2\sigma_0^2}\right) \left(\frac{\left(\frac{d}{dt_i}\beta - \frac{d}{dt_i}\mu_0\right)\sigma_0 - \left(\frac{d}{dt_i}\sigma_0\right)(\beta - \mu_0)}{\sigma_0^2}\right) \\ - \exp\left(\frac{-(\beta - \mu_1)^2}{2\sigma_1^2}\right) \left(\frac{\left(\frac{d}{dt_i}\beta - \frac{d}{dt_i}\mu_1\right)\sigma_1 - \left(\frac{d}{dt_i}\sigma_1\right)(\beta - \mu_1)}{\sigma_1^2}\right) = 0. \end{aligned} \quad (80)$$

Let $g_{i,l} = \frac{d}{dt_i} \lambda_{i,l}$. Hence, from definition of β and w_l in Corollary 2.1, we have $\frac{d}{dt_i} \beta = g_{0,l} - g_{1,l}$ and

$$\frac{d}{dt_i} \mu_i = \left(\frac{g_{0,l}}{\lambda_{0,l}} - \frac{g_{1,l}}{\lambda_{1,l}}\right) \lambda_{i,l} + w_l g_{i,l}, \quad \frac{d}{dt_i} \sigma_i = \frac{w_l}{2\sigma_i} \left[2\left(\frac{g_{0,l}}{\lambda_{0,l}} - \frac{g_{1,l}}{\lambda_{1,l}}\right) \lambda_{i,l} + w_l g_{i,l}\right], \quad i = 0, 1. \quad (81)$$

Hence, we obtain the set of equations in (46). For the location invariant flow and transparent receiver, $\lambda_{i,l} = V_R \zeta h_0(\mathbf{r}_0 - \int_{t_0}^{t_l} \mathbf{v}_i(\tau) d\tau, t)$. Using (7), we have

$$\begin{aligned} g_{i,l} &= V_R \zeta \frac{d}{dt_l} h_0(\mathbf{r}_0 - \int_{t_r}^{t_l} \mathbf{v}_i(\tau) d\tau, t_l) = V_R \zeta \frac{d}{dt_l} \left[\frac{1}{(4\pi D(t_l - t_r))^{\frac{3}{2}}} e^{-\frac{\|\mathbf{r}_0 - \int_{t_r}^{t_l} \mathbf{v}_i(\tau) d\tau\|^2}{4D(t_l - t_r)}} \right] \\ &= \lambda_{i,l} \left[\frac{-3}{2(t_l - t_r)} + \frac{\langle \mathbf{v}_i(t_l), \mathbf{r}_0 - \int_{t_r}^{t_l} \mathbf{v}_i(\tau) d\tau \rangle}{2D(t_l - t_r)} + \frac{\|\mathbf{r}_0 - \int_{t_r}^{t_l} \mathbf{v}_i(\tau) d\tau\|^2}{4D(t_l - t_r)^2} \right]. \end{aligned} \quad (82)$$

APPENDIX D
PROOF OF LEMMA 7

To obtain the sub-optimum sampling times using (30), we should solve

$$\max_{t_1, \dots, t_L} \max_s \sum_{l=1}^L [\lambda_{0,l}s + \lambda_{1,l}(1-s) - \lambda_{0,l}^s \lambda_{1,l}^{1-s}]. \quad (83)$$

Let $f(t_l, s) = \lambda_{0,l}s + \lambda_{1,l}(1-s) - \lambda_{0,l}^s \lambda_{1,l}^{1-s}$. Hence, the optimum values of t_1, \dots, t_L , and s are the solutions of $\nabla \sum_{l=1}^L f(t_l, s) = [\frac{\partial f(t_1, s)}{\partial t_1}, \dots, \frac{\partial f(t_L, s)}{\partial t_L}, \sum_{l=1}^L \frac{\partial f(t_l, s)}{\partial s}] = 0$. From $\frac{\partial f(t_l, s)}{\partial t_l} = 0, l = 1, \dots, L$, we conclude that $t_1 = t_2 = \dots = t_L$. Hence, from $\sum_{l=1}^L \frac{\partial f(t_l, s)}{\partial s} = 0$, we obtain $\frac{\partial f(t_1, s)}{\partial s} = 0$. Thus, s and t_1 are the solutions of $[\frac{\partial f(t_1, s)}{\partial t_1}, \frac{\partial f(t_1, s)}{\partial s}] = 0$. This means that the sub-optimum values of t_1, \dots, t_L are equal to the values when $L = 1$.

Now, we obtain the set of equations for the sub-optimum sampling time when $L = 1$, i.e., t_1 . From (35), which is the solution of $\frac{\partial f(t_1, s)}{\partial s} = 0$, we have $s = \frac{\ln(\frac{\lambda_{0,1}}{\lambda_{1,1}} - 1) - \ln \ln(\frac{\lambda_{0,1}}{\lambda_{1,1}})}{\ln(\frac{\lambda_{0,1}}{\lambda_{1,1}})}$. Further, $\frac{\partial f(t_1, s)}{\partial t_1} = 0$ yields to

$$g_{0,1}s + g_{1,1}(1-s) - sg_{0,1}(\frac{\lambda_{1,1}}{\lambda_{0,1}})^{1-s} - (1-s)g_{1,1}(\frac{\lambda_{0,1}}{\lambda_{1,1}})^s = 0,$$

where $g_{i,l}$ is defined in Lemma 6.

APPENDIX E
PROOF OF CORROLARY 8.1

For $\mathbf{v} = v\mathbf{d}$, and uniform distribution for v , the map estimation of v is

$$\hat{v} = \arg \max_{v_{\min} \leq v \leq v_{\max}} y_1 \ln(\lambda_1(v\mathbf{d})) - \lambda_1(v\mathbf{d}). \quad (84)$$

In the following, let $R_{\text{est},u}(v) = y_1 \ln(\lambda_1(v\mathbf{d})) - \lambda_1(v\mathbf{d})$. Hence, we should find the solutions of $R'_{\text{est},u}(v) = \frac{d}{dv} R_{\text{est},u}(v) = 0$ which maximize $R_{\text{est},u}(v)$ and fall in S_v . For the transparent receiver, we have $R'_{\text{est},u}(v) = \frac{1}{2D}(r_0 - v \cdot (t_1 - t_r)) \cdot (y_1 - \lambda_1(v\mathbf{d})) = 0$. If there is no maximizer in this range, we should consider v_{\min}, v_{\max} . Hence, the candidates of the maximizer are the values of v which satisfy the equations $r_0 - v \cdot (t_1 - t_r) = 0$ and $\lambda_1(v\mathbf{d}) = y_1$. From $r_0 - v \cdot (t_1 - t_r) = 0$, we obtain $v_1 = \frac{r_0}{t_1 - t_r}$. Note that v_1 maximizes $\lambda_1(v\mathbf{d})$, i.e., $\lambda_1(v\mathbf{d})$ is a positive function with maximum $\lambda_1(v_1\mathbf{d}) = \frac{\zeta V_R}{(4\pi D(t_1 - t_r))^{\frac{3}{2}}}$. For the second equation, we have three cases:

Case 1) $y_1 = \lambda_1(v_1\mathbf{d})$: in this case, the only solution of the equation $\lambda_l(v_1\mathbf{d}) = y_1$ is equal to v_1 .

Case 2) $y_1 > \lambda_1(v_1\mathbf{d})$: in this case, the second equation $\lambda_l(v\mathbf{d}) = y_1$ does not have any solutions for v since y_l is greater than the maximum value of $\lambda_l(v\mathbf{d})$.

Case 3) $y_1 < \lambda_1(v_1\mathbf{d})$: in this case, the equation $\lambda_l(v\mathbf{d}) = y_1$ has two solutions as follows:

$$v_2 = \frac{r_0 + \sqrt{-4D(t_1 - t_r)(\ln y_1 - \ln(\lambda_1(v_1\mathbf{d}))}}{t_1 - t_r}, \quad v_3 = \frac{r_0 - \sqrt{-4D(t_1 - t_r)(\ln y_1 - \ln(\lambda_1(v_1\mathbf{d}))}}{t_1 - t_r}.$$

In Case 1, we have $R'_{\text{est,u}}(v) = \frac{1}{2D}(r_0 - v.(t_1 - t_r)).(\lambda_1(v_1\mathbf{d}) - \lambda_1(v\mathbf{d}))$. Since v_1 is the maximizer of $\lambda_1(v_1\mathbf{d})$, $\lambda_1(v_1\mathbf{d}) - \lambda_1(v\mathbf{d})$ is positive for all $v \neq v_1$. Hence, for $v < v_1$, $R'_{\text{est,u}}(v) > 0$ and for $v > v_1$, $R'_{\text{est,u}}(v) < 0$, and thus, v_1 is the maximizer. Now, using the second derivative of $R_{\text{est,u}}(v)$, we show that in Case 2, v_1 is the only maximizer of $R_{\text{est,u}}(v)$ and in Case 3, v_1 is the minimizer and v_2 and v_3 are the maximizers of $R_{\text{est,u}}(v)$, and if both values fall in S_v , the estimator gives one of the values v_2 and v_3 randomly as the estimated value of v .

The second derivative of $R_{\text{est}}(v)$ can be obtained as

$$R''_{\text{est,u}}(v) = \frac{d^2}{dv^2}R_{\text{est,u}}(v) = -\frac{1}{2D}(t_1 - t_r)(y_1 - \lambda_1(v\mathbf{d})) - \frac{1}{4D^2}(r_0 - v.(t_1 - t_r))^2\lambda_1(v\mathbf{d}). \quad (85)$$

For $v = v_1$, we have $r_0 - v.(t_1 - t_r) = 0$ and hence,

$$R''_{\text{est,u}}(v) = -(t_1 - t_r)(y_1 - \lambda_1(v\mathbf{d})). \quad (86)$$

Now in Case 2, we have $R''_{\text{est,u}}(v_1) < 0$, and hence, v_1 is the maximizer. In Case 3, we have $R''_{\text{est,u}}(v_1) > 0$, and hence, v_1 is the minimizer.

For v_2 and v_3 in Case 3, we have $y_1 = \lambda_1(v\mathbf{d})$ and hence,

$$R''_{\text{est,u}}(v) = -\frac{1}{4D^2}(r_0 - v.(t_1 - t_r))^2\lambda_1(v\mathbf{d}). \quad (87)$$

Since $(r_0 - v.(t_1 - t_r))^2 > 0$ and $\lambda_l(\mathbf{v})$ is a positive function, $R''_{\text{est,u}}(v)|_{v=v_1,v_2} < 0$ and hence, v_2 and v_3 are the maximizers.

APPENDIX F

PROOF OF LEMMA 9

For the MMSE estimator, when the mean and variance of $v_i, i \in \{x, y, z\}$ is finite, we have [39]

$$\hat{v}_i = E[v_i|y_1, \dots, y_L]. \quad (88)$$

for \hat{v}_x we have

$$P(v_x|y_1, \dots, y_L) = \frac{P(y_1, \dots, y_L|v_x)p_x(v_x)}{P(y_1, \dots, y_L)} = \frac{p_x(v_x) \int_{v_y, v_z} p_y(v_y)p_z(v_z)P(y_1, \dots, y_L|v_x, v_y, v_z)dv_zdv_y}{\int p_x(v_x)p_y(v_y)p_z(v_z)P(y_1, \dots, y_L|v_x, v_y, v_z)dv_zdv_ydv_x}. \quad (89)$$

For the independent observations, we have

$$P(v_x|y_1, \dots, y_L) = \frac{p_x(v_x) \int_{v_y, v_z} p_y(v_y)p_z(v_z)\prod_{l=1}^L P(y_l|v_x, v_y, v_z)dv_zdv_y}{\int p_x(v_x)p_y(v_y)p_z(v_z)\prod_{l=1}^L P(y_l|v_x, v_y, v_z)dv_zdv_ydv_x}. \quad (90)$$

Therefore,

$$\hat{v}_x = E(v_x|y_1, \dots, y_L) = \frac{\int_{v_x} v_x p_x(v_x) \int_{v_y, v_z} p_y(v_y)p_z(v_z)\prod_{l=1}^L P(y_l|\mathbf{v})dv_zdv_ydv_x}{\int p_x(v_x)p_y(v_y)p_z(v_z)\prod_{l=1}^L P(y_l|\mathbf{v})dv_zdv_ydv_x}. \quad (91)$$

Let $p_{x,y,z}(\mathbf{v}) = p_x(v_x)p_y(v_y)p_z(v_z)$. Since the conditional probability distribution of $Y_l, l = 1, \dots, L$ given \mathbf{v} is $\text{Poiss}(\lambda_l(\mathbf{v}))$, we obtain the equation (54).

For the LMMSE, the estimator of \mathbf{v} can be obtained as

$$\hat{\mathbf{v}} = \mathbf{y}A + \mathbf{b}, \quad (92)$$

where $A = C_{YY}^{-1}C_{Y\mathbf{v}}$, $\mathbf{y} = (y_1, y_2, \dots, y_L)$, $\mathbf{b} = \boldsymbol{\mu} - \boldsymbol{\lambda}A$, in which

$$\boldsymbol{\mu} = \mathbb{E}[\mathbf{v}] = (\mathbb{E}[v_x], \mathbb{E}[v_y], \mathbb{E}[v_z]), \quad \boldsymbol{\lambda} = (\mathbb{E}[Y_1], \mathbb{E}[Y_2], \dots, \mathbb{E}[Y_L]), \quad (93)$$

$$C_{YY} = \begin{bmatrix} \text{Var}(Y_1) & \text{Cov}(Y_1, Y_2) & \dots & \text{Cov}(Y_1, Y_L) \\ \text{Cov}(Y_2, Y_1) & \text{Var}(Y_2) & \dots & \text{Cov}(Y_2, Y_L) \\ \vdots & \vdots & \ddots & \vdots \\ \text{Cov}(Y_L, Y_1) & \text{Cov}(Y_L, Y_2) & \dots & \text{Var}(Y_L) \end{bmatrix}, \quad C_{Y\mathbf{v}} = \begin{bmatrix} \text{Cov}(Y_1, v_x) & \text{Cov}(Y_1, v_y) & \text{Cov}(Y_1, v_z) \\ \text{Cov}(Y_2, v_x) & \text{Cov}(Y_2, v_y) & \text{Cov}(Y_2, v_z) \\ \vdots & \vdots & \vdots \\ \text{Cov}(Y_L, v_x) & \text{Cov}(Y_L, v_y) & \text{Cov}(Y_L, v_z) \end{bmatrix}.$$

Now, since the observations are assumed to be independent, we have $\text{Cov}(Y_{l_1}, Y_{l_2}) = 0$, for $l_1 \neq l_2$.

Hence it is straightforward to obtain (55).

APPENDIX G

PROOF OF LEMMA 10

We obtain the matrixes J_D and J_P in the BCR lower bound given in (61), (62). The (i, j) -th entry of J_P can be obtained as

$$\{J_P\}_{i,j} = -\mathbb{E}_{\mathbf{v}}\left[\frac{\partial^2}{\partial v_i \partial v_j} \ln(p_{x,y,z}(\mathbf{v}))\right] = -\mathbb{E}_{\mathbf{v}}\left[\frac{\partial^2}{\partial v_i \partial v_j} (\ln(p_x(v_x)) + \ln(p_y(v_y)) + \ln(p_z(v_z)))\right]. \quad (94)$$

Hence, it is straightforward to obtain (66). The (i, j) -th entry of the matrix $J_F(\mathbf{v})$ is obtained as

$$\{J_F(\mathbf{v})\}_{i,j} = -\mathbb{E}_{\mathbf{Y}|\mathbf{v}}\left[\frac{\partial^2}{\partial v_i \partial v_j} \left(\sum_{l=1}^L \ln(P(Y_l|\mathbf{v}))\right)\right] = -\sum_{l=1}^L \mathbb{E}_{\mathbf{Y}|\mathbf{v}}\left[\frac{\partial^2}{\partial v_i \partial v_j} (Y_l \ln(\lambda_l(\mathbf{v})) - \lambda_l(\mathbf{v}))\right], \quad (95)$$

which can be simplified to

$$\{J_F(\mathbf{v})\}_{i,j} = -\sum_{l=1}^L \mathbb{E}_{\mathbf{y}|\mathbf{v}}\left[\left(\frac{\partial}{\partial v_i} \left[\frac{1}{\lambda_l(\mathbf{v})} \cdot \frac{\partial \lambda_l(\mathbf{v})}{\partial v_j}\right]\right)(y_l - \lambda_l(\mathbf{v})) + \left(\frac{1}{\lambda_l(\mathbf{v})} \cdot \frac{\partial \lambda_l(\mathbf{v})}{\partial v_j}\right)\left(-\frac{\partial \lambda_l(\mathbf{v})}{\partial v_i}\right)\right]. \quad (96)$$

Now, since $\mathbb{E}_{Y_l|\mathbf{v}}[Y_l] = \lambda_l(\mathbf{v})$ and the second term is not related to \mathbf{y} , we have

$$\{J_F(\mathbf{v})\}_{i,j} = \sum_{l=1}^L \frac{1}{\lambda_l(\mathbf{v})} \cdot \frac{\partial \lambda_l(\mathbf{v})}{\partial v_j} \frac{\partial \lambda_l(\mathbf{v})}{\partial v_i}. \quad (97)$$

Hence, the (i, j) -th entry of the matrix $J_D = \mathbb{E}_{\mathbf{v}}[J_F(\mathbf{v})]$ is obtained as (65).